EUROfusion

A model of non-Maxwellian electron distribution for the analysis of ECE in JET discharges

G. Giruzzi (CEA, IRFM, France)

JET

This work has been carried out within the framework of the EUROfusion Consortium, funded by the European Union via the Euratom Research and Training Programme (Grant Agreement No 101052200 — EUROfusion). Views and opinions expressed are however those of the author(s) only and do not necessarily reflect those of the European Union or the European Commission. Neither the European Union nor the European Commission can be held responsible for them.

Outline

- What **is seen** by ECE harmonics and by Thomson scattering
- Evidence of **non-Maxwellian electron distributions** in JET high-T_e database (M. Fontana's talk)
- **ECE sets constraints** on the electron distribution function
- **Toy model** of perturbed electron distribution function: a data analysis tool
- Model-experiment **comparison**
- Conclusions. Possible **interpretations**

Note: this work continues and develops previous analyses made by E. De la Luna and V. Krivenski:

- *E. de la Luna et al., Rev. Sci. Instr.* ***74****, 1414 (2003)*
- *V. Krivenski, Fus. Eng. Des.* ***53****, 23 (2001)*

G. Giruzzi[1], M. Fontana[2], F.P. Orsitto[3] , E. de la Luna[4] , R. Dumont[1], L. Figini[5], M. Maslov[2], S. Mazzi[6], S. Schmuck[5], L. Senni[3], C. Sozzi[5], C. Challis[2], D. Frigione[3], J. Garcia[1], L. Garzotti[2], J. Hobirk[7], A. Kappatou[7], D. Keeling[2], E. Lerche[2], C. Maggi[2], J. Mailloux[2], F. Rimini[2], D. Van Eester[8], and JET contributors

[1] CEA, IRFM, France [2] CCFE, Culham Science Centre, UK [3] ENEA, C R Frascati, Italy [4] National Fusion Laboratory, CIEMAT, Madrid, Spain [5] ISTP, CNR, Milano, Italy [6] EPFL, Swiss Plasma Center, Lausanne, Switzerland [7] Max-Planck-Institut für Plasmaphysik, Garching, Germany [8] Laboratory for Plasma Physics, LPP-ERM/KMS, Brussels, Belgium

ECE (harmonic *n*, X-mode, perpendicular propagation)

Radiation temperature

$$T_{rad}(\omega) = \int_{R_0-a}^{R_0+a} dR\, \beta(R)\, exp\left(-\int_R^{R_0+a} \alpha(R')dR'\right)$$

Optical depth

$$\tau = \int_{R_0-a}^{R_0+a} \alpha(R)dR$$

absorption coefficient: $\alpha \propto \int d\vec{p}\; p_\perp^{2n-1} \frac{\partial f}{\partial p_\perp} \delta(\gamma - n\frac{\omega_c}{\omega})$

emission coefficient: $\beta \propto \int d\vec{p}\, \frac{p_\perp^{2n}}{\gamma} f\, \delta(\gamma - n\frac{\omega_c}{\omega})$ $\quad \vec{p} = \mathrm{m}\gamma\vec{v}$

for a **Maxwellian:** $\beta = T_e\alpha$ (**Kirchhoff's law** → plasma is a black body)

$\omega = \frac{n\omega_c(R)}{\gamma}$, $\gamma = \sqrt{1 + \frac{p^2}{(mc)^2}}$, cold resonance position: $n\omega_c(R_c) = \omega$

kinetic energy: $E_k = mc^2(\gamma - 1) = mc^2\left(\frac{R_c}{R} - 1\right)$

What is seen by 2nd harmonic ECE and by Thomson (in energy)

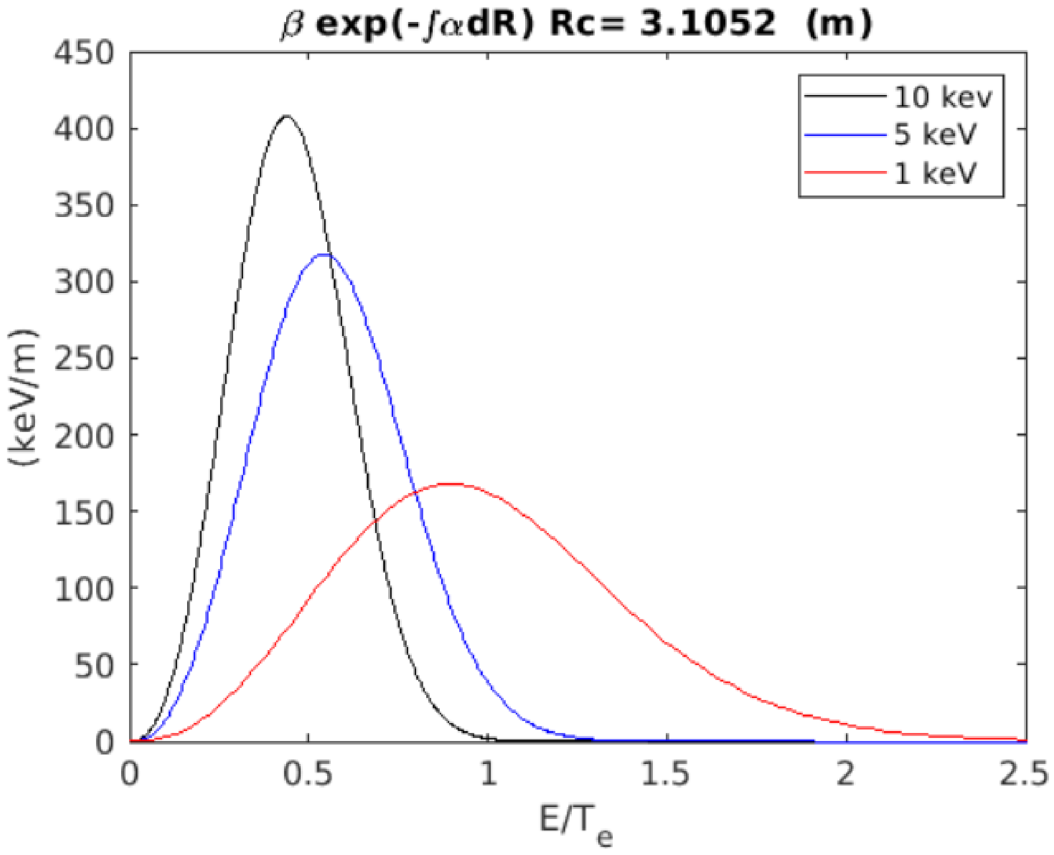

From S.L. Prunty 2014 *Phys. Scr.* **89** 128001, Eqs. 5.8, 5.9 (neglecting depolarisation effect):

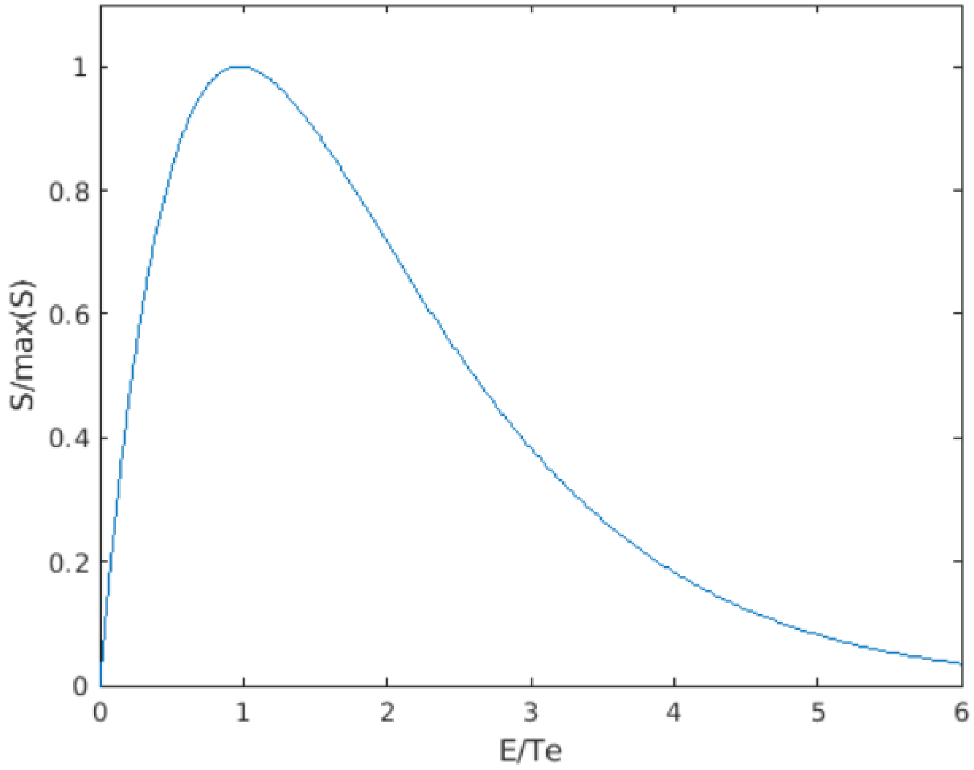

$$S \propto \frac{\left(\frac{v}{c}\right)^2}{\left(1-\left(\frac{v}{c}\right)^2\right)^{3/2}} exp\left(-\frac{mc^2/T_e}{\left(1-\left(\frac{v}{c}\right)^2\right)^{1/2}}\right)$$

2^{nd} & 3^{rd} harmonics see different momenta → constraints on *f(p)*

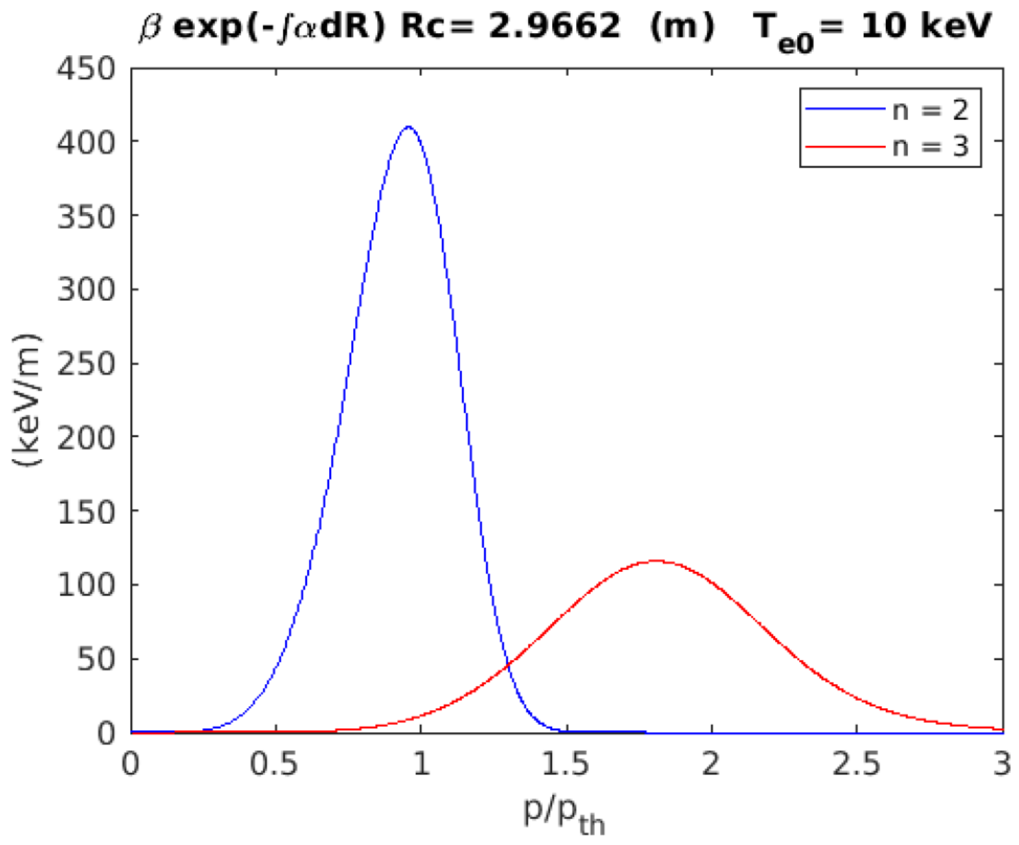

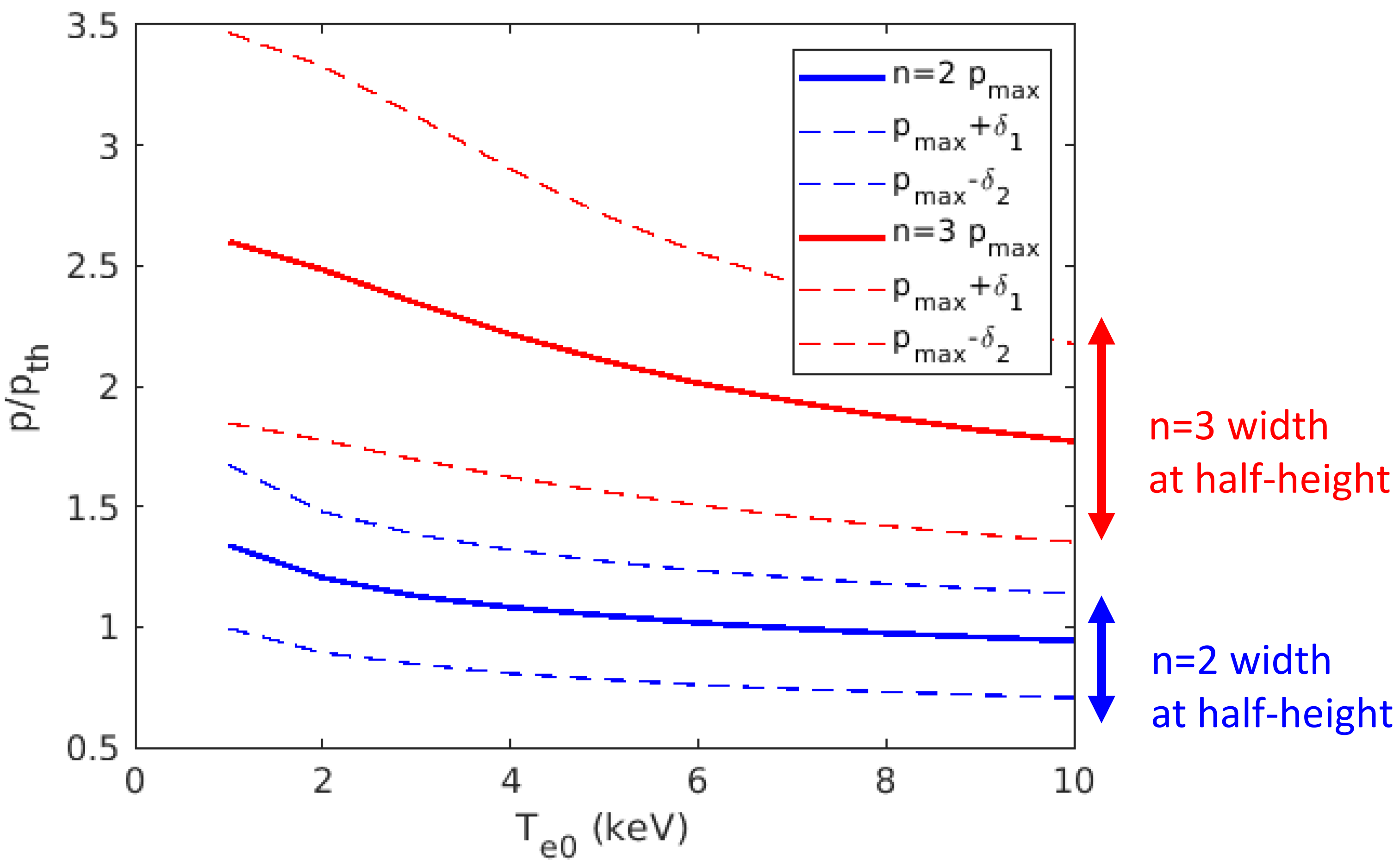

$$p_{th} = mv_{th}$$

T_{e0} database (~230 pulses, ~12000 time slices) by M. Fontana

Maxwellian predictions and data

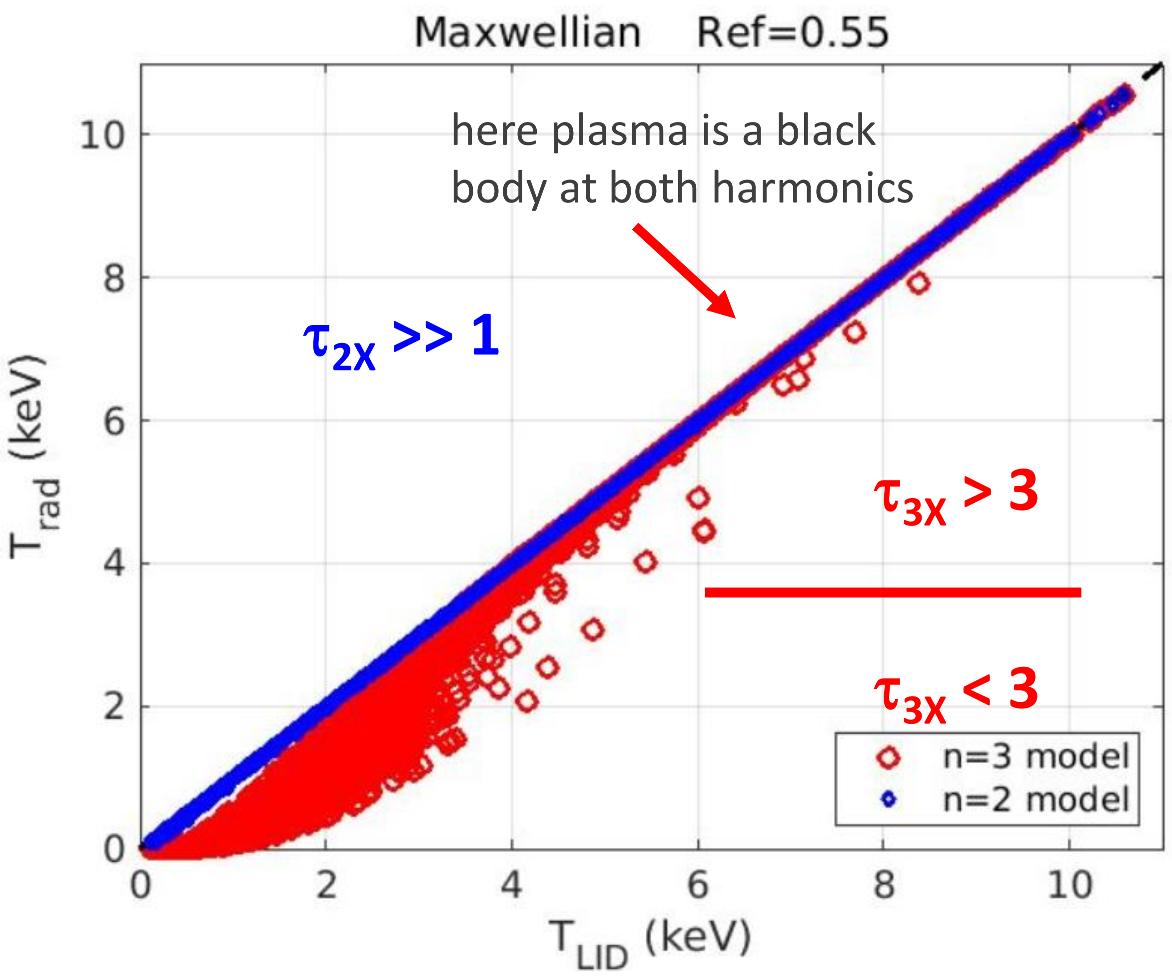

Maxwellian predictions and data

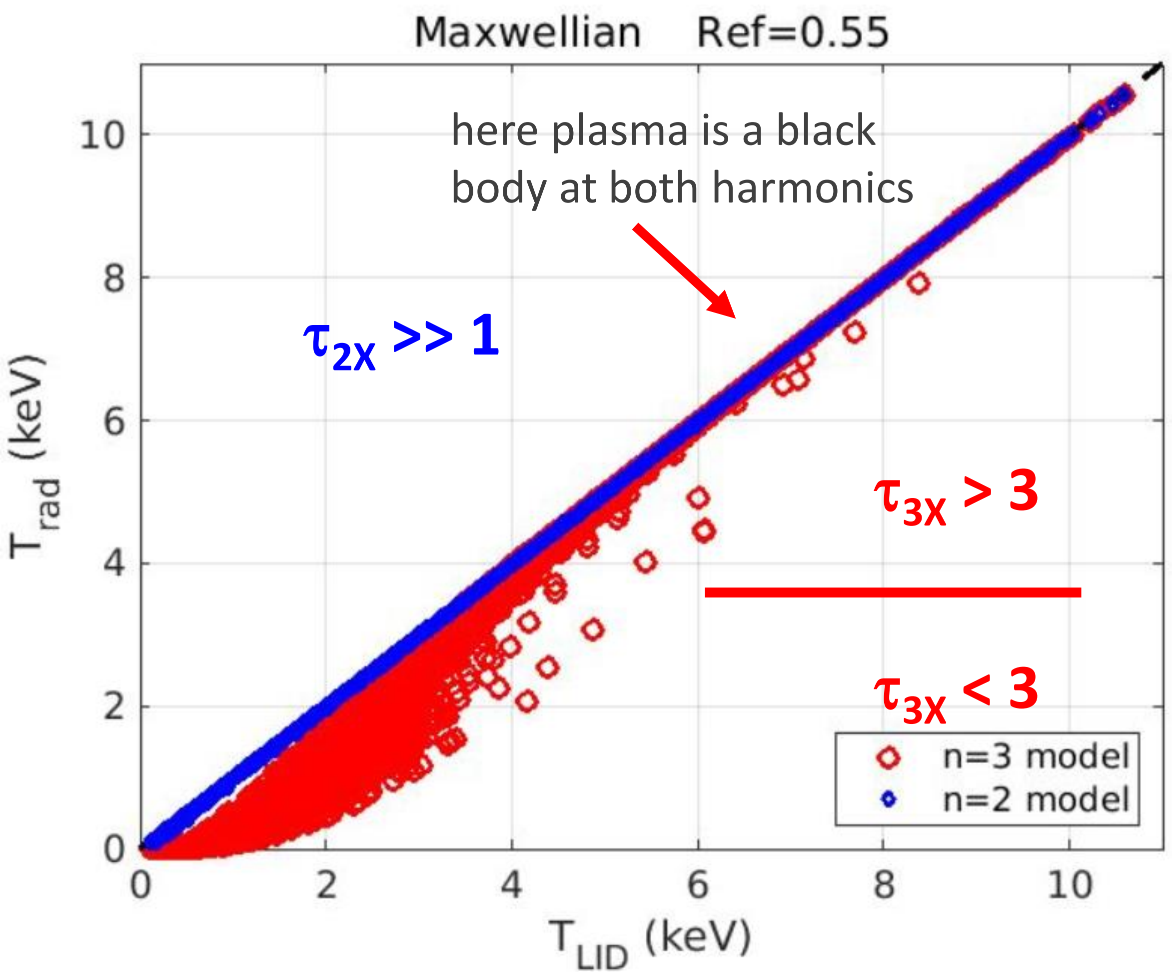

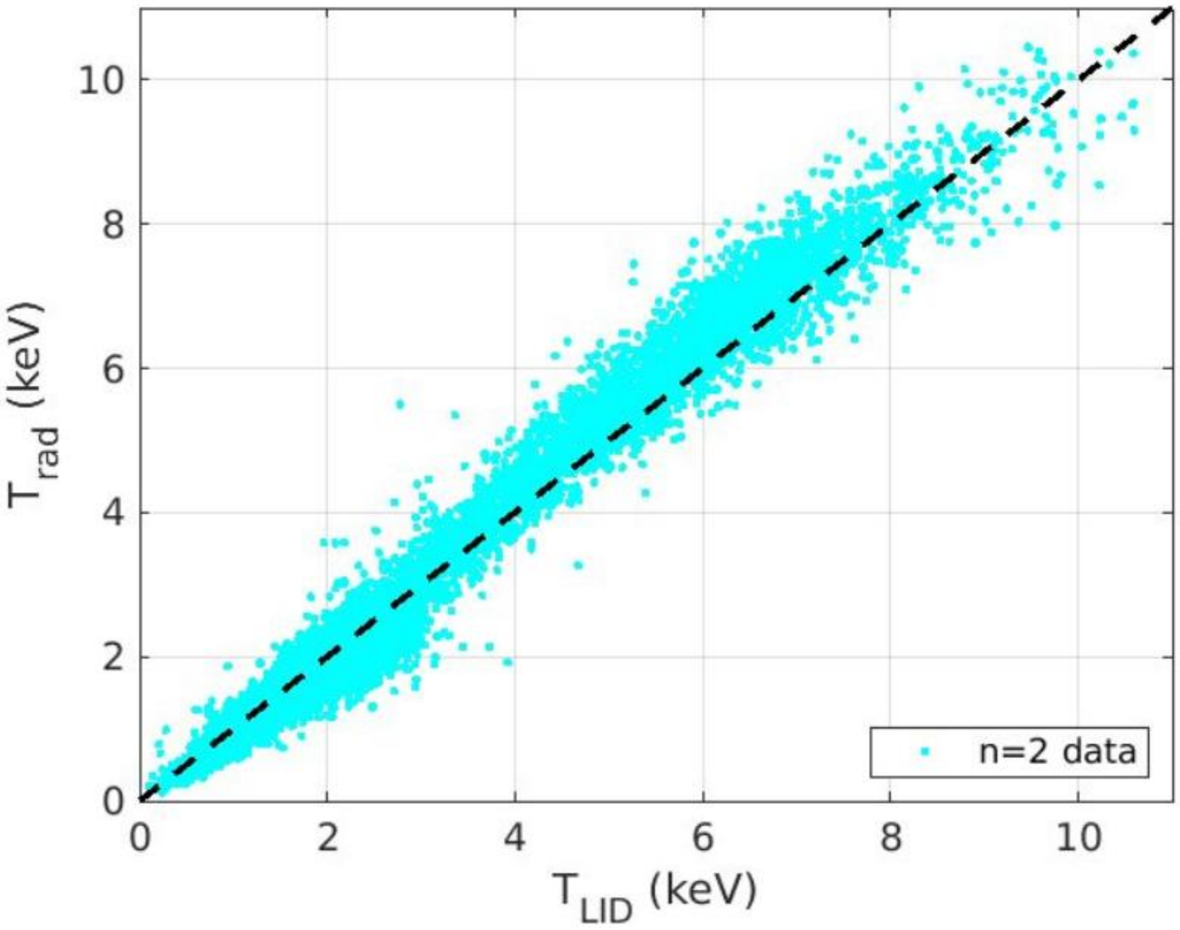

T_{e0} database (~230 pulses, ~12000 time slices) by M. Fontana

Maxwellian predictions and data

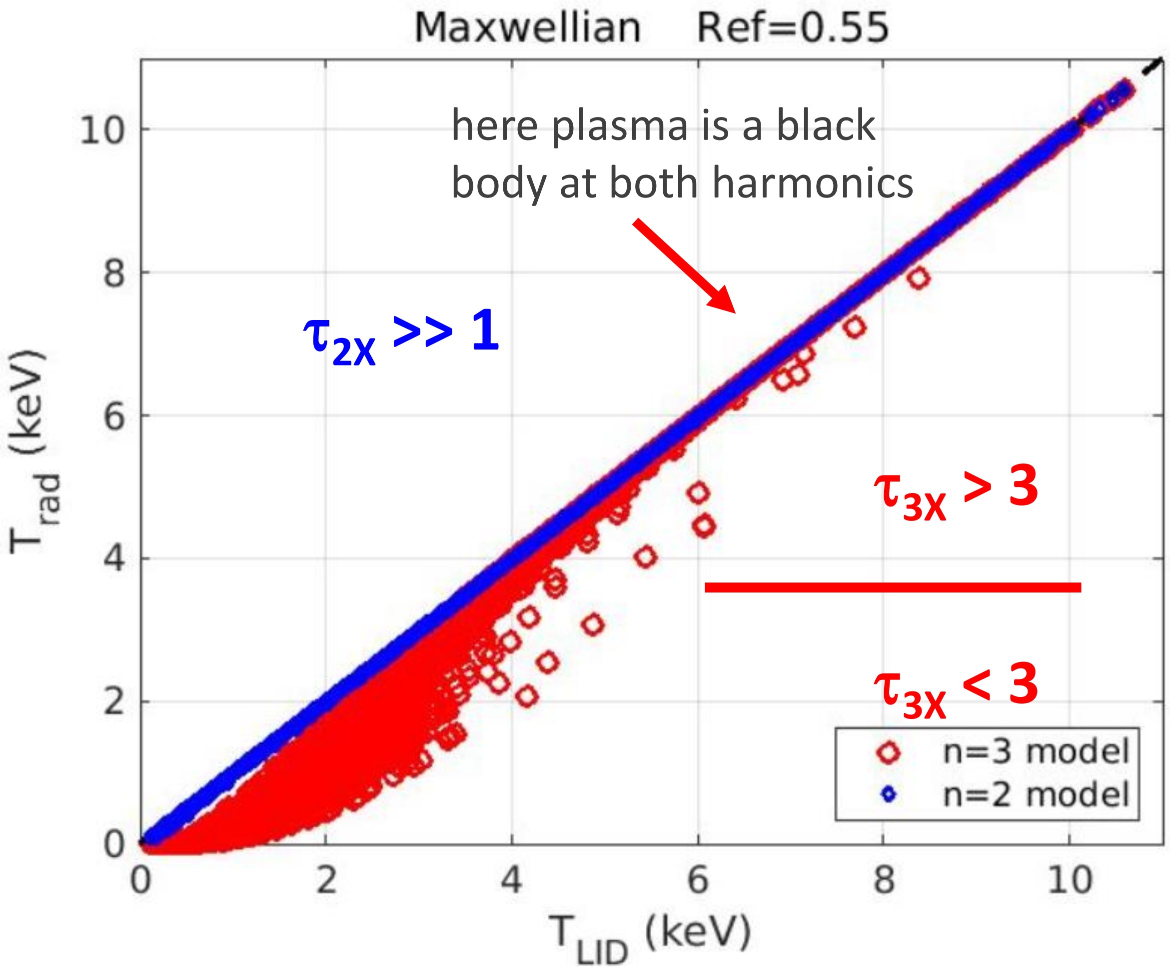

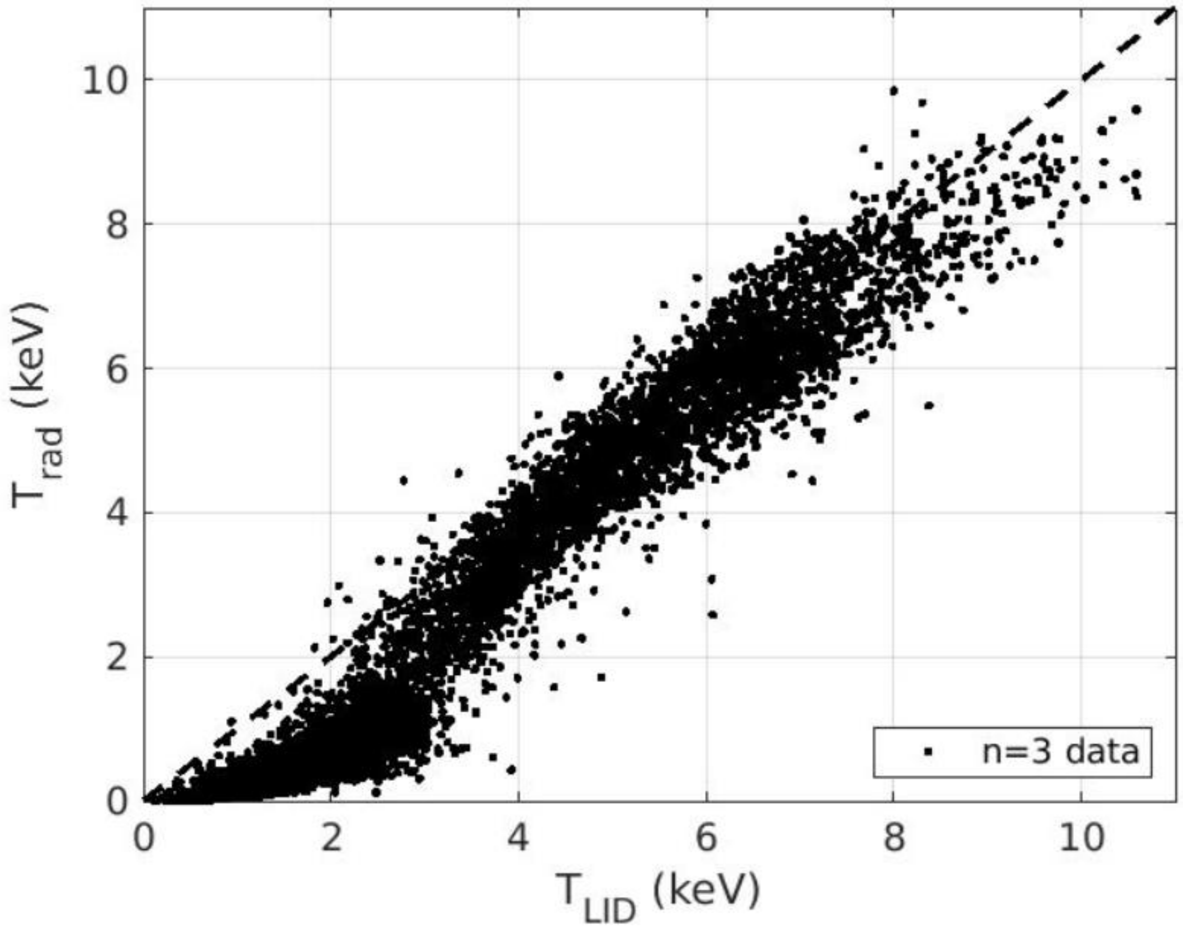

T_{e0} database (~230 pulses, ~12000 time slices) by M. Fontana

Maxwellian predictions and data

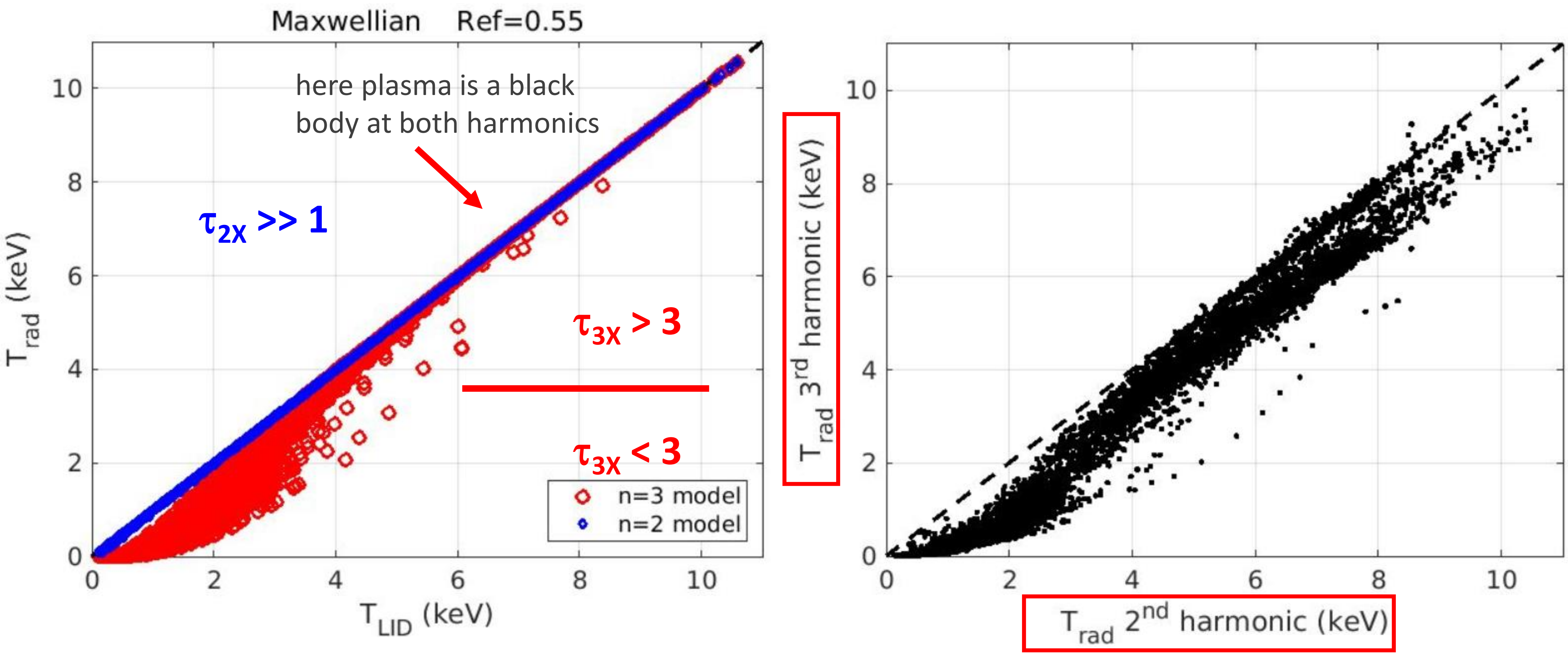

Maxwellian predictions and data

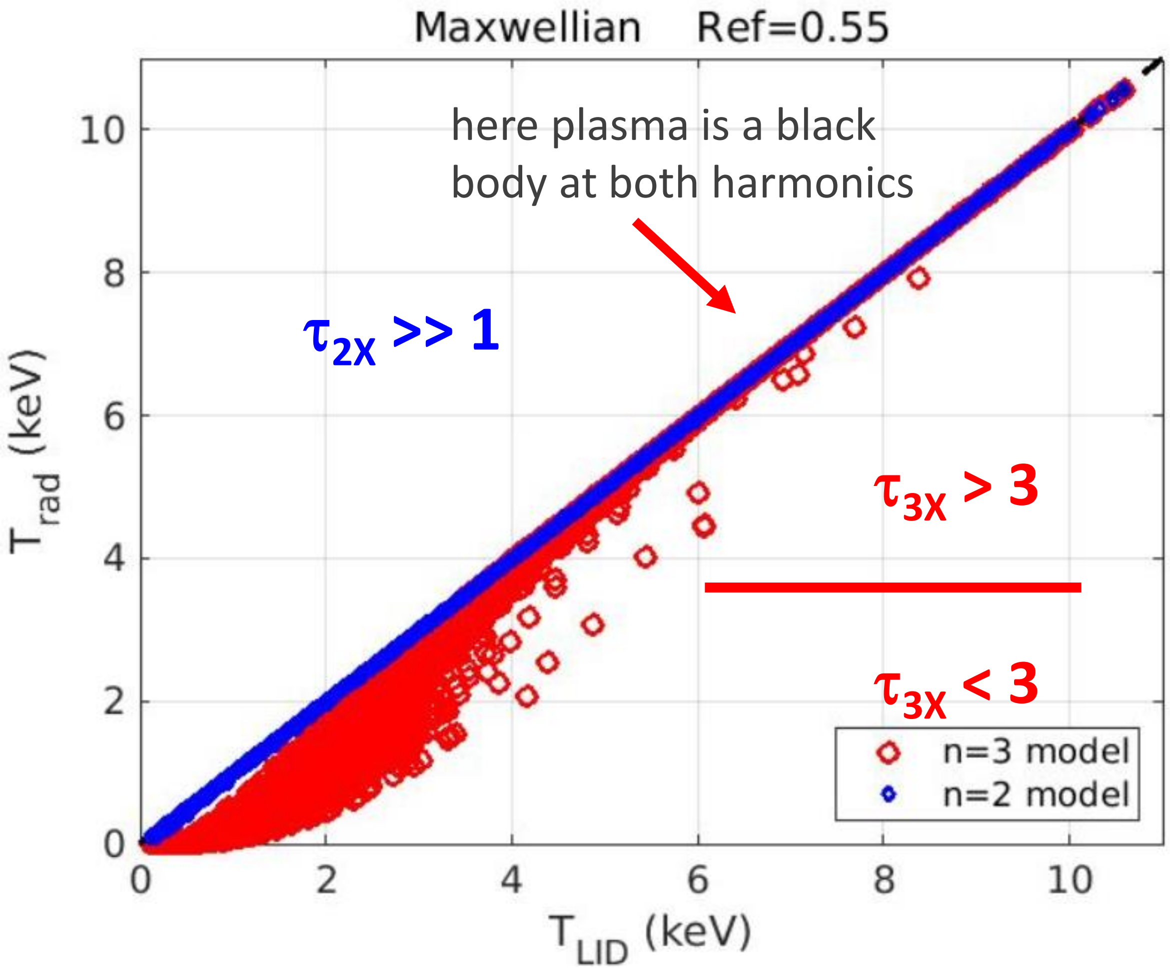

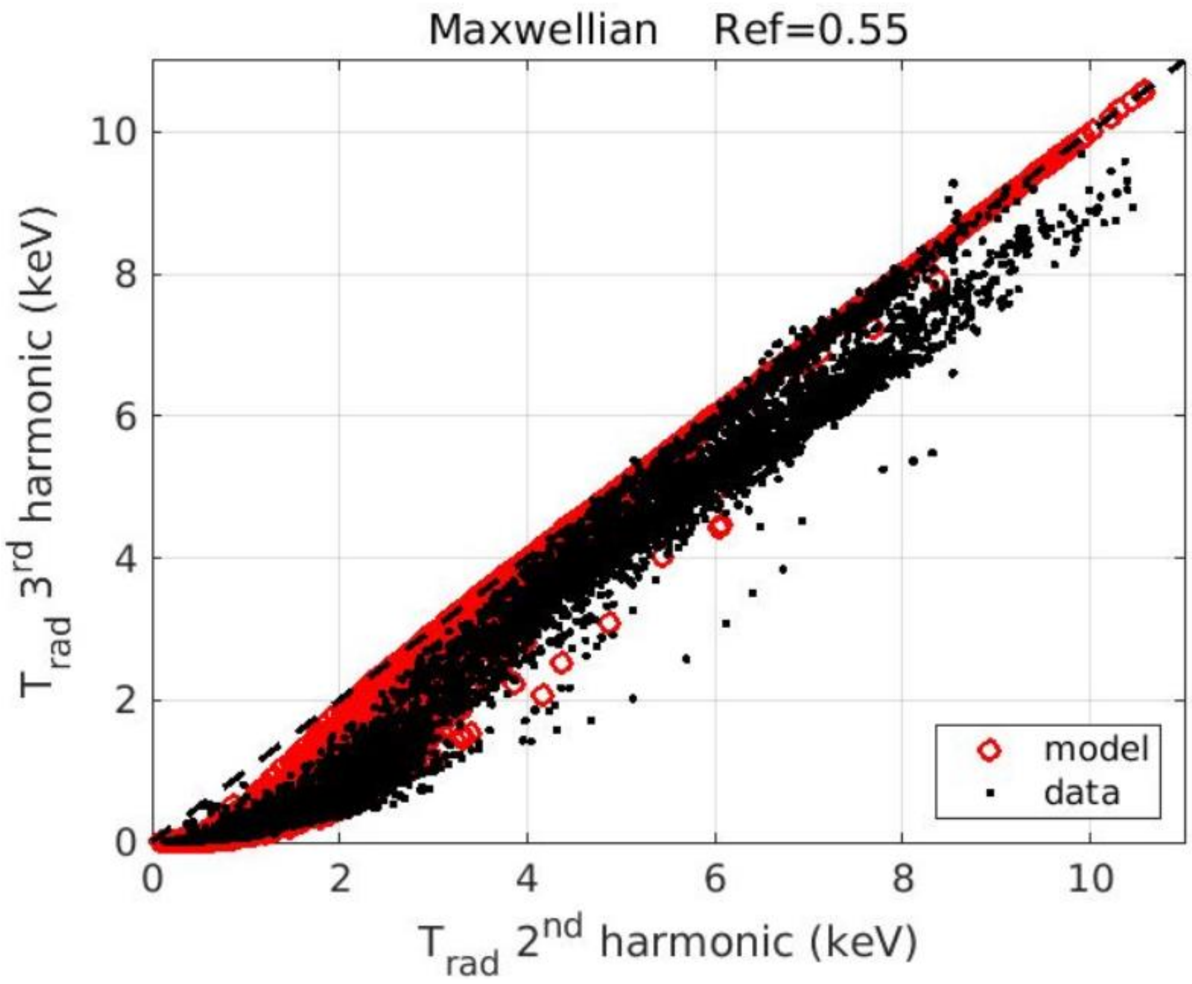

Toy model of perturbed electron distribution function

Relativistic Maxwellian distribution in momentum p:

$$f_M = Ae^{-\mu(\gamma-1)} \qquad A = \frac{\mu e^{-\mu}}{4\pi K_2(\mu)(mc)^3} \qquad \mu = \frac{mc^2}{T_e}$$

Perturbed distribution:

$$f = A(e^{-\mu(\gamma-1)} + f_1)$$

Bipolar isotropic perturbation:

$$f_{1u} = f_0 sin\left[\frac{\pi}{\delta}(p-p_0)\right] \quad \text{for} \quad p_0 - \delta < p < p_0 + \delta$$

Some anisotropic perturbations (θ = pitch-angle), examples:

$$f_{1s} = f_{1u} sin\theta \qquad f_{1c2} = f_{1u} cos^2\theta$$

$$f_{1s2} = f_{1u} sin^2(2\theta) \qquad f_{1c} = f_{1u} cos\theta$$

All these functions allow analytical calculation of EC absorption and emission coefficients.

In the following, only the isotropic perturbation is used

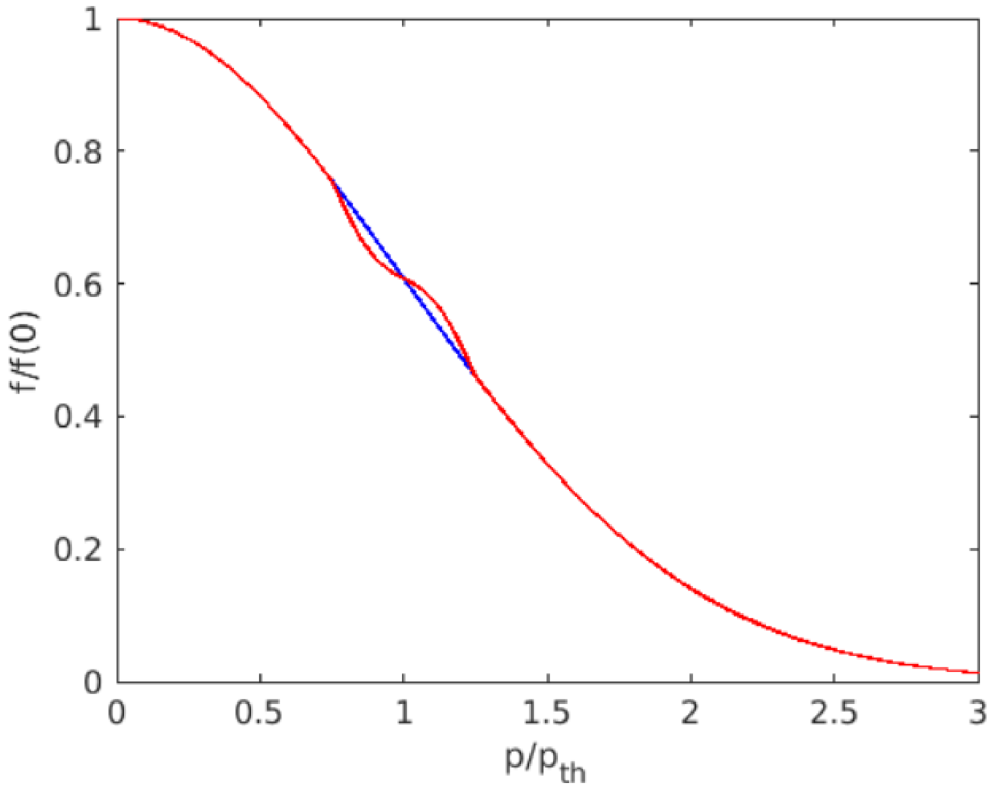

$f_0 = 0.03$ $\quad p_0/p_{th} = 1$ $\quad \delta/p_{th} = 0.25$

↑ intensity ↑ location ↑ width

Different perturbation locations and widths → different effects

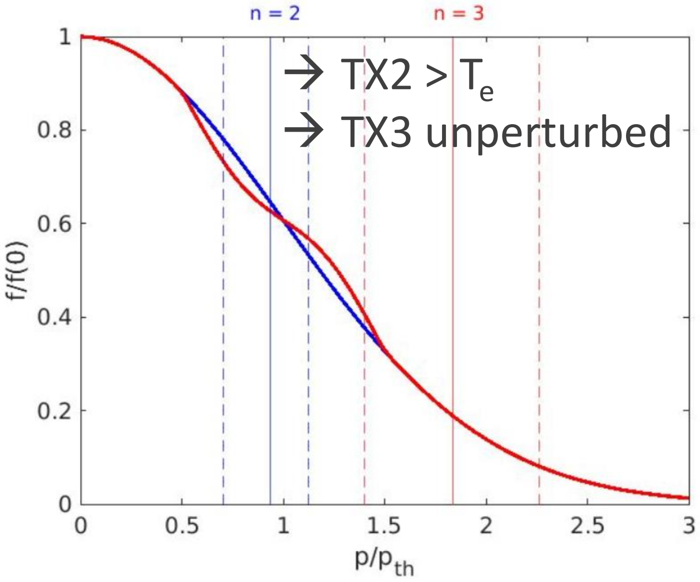

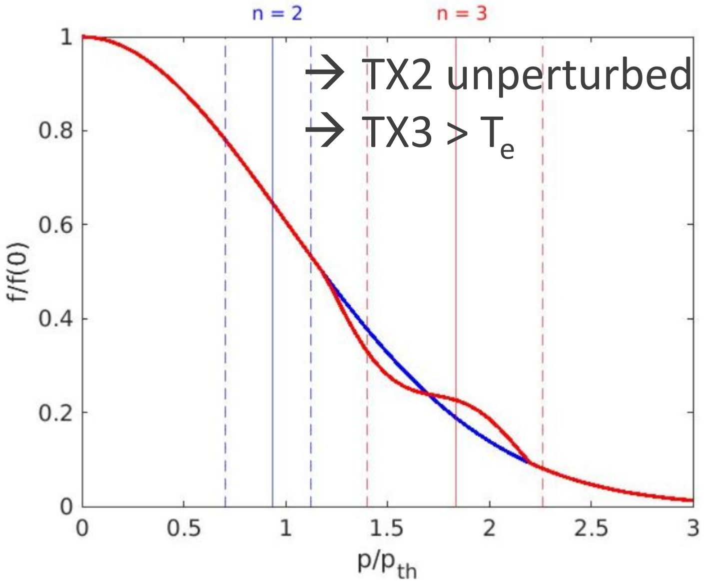

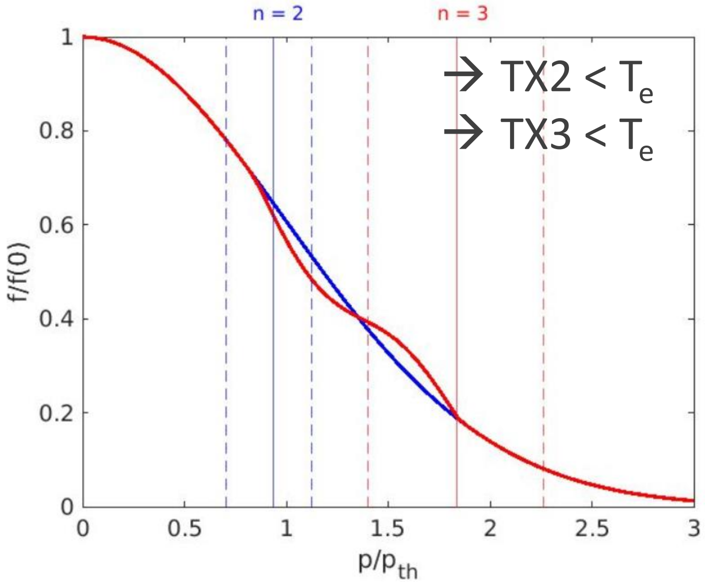

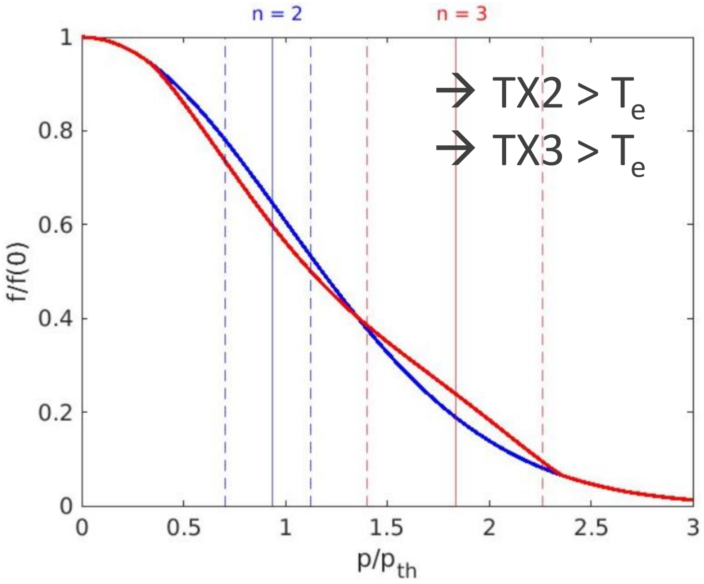

Various possibilities depending on perturbation location and width:

- TX2 > T_e and TX3 < T_e (most usual one)
- TX2 Maxwellian and TX3 non-Maxwellian
- TX2 non-Maxwellian and TX3 Maxwellian
- both TX2 and TX3 < T_e
- both TX2 and TX3 > T_e

Absorption and emission coefficients of X mode

$$\boldsymbol{\alpha} = \boldsymbol{A_0} \sum_{\boldsymbol{n}} \boldsymbol{\alpha_n} \qquad \alpha_n = A_n \left[\frac{\mu u_n}{n\omega_c/\omega} e^{-\mu\left(\frac{n\omega_c}{\omega}-1\right)} - Q_n h(u_n) \frac{\pi}{\delta/mc} f_0 cos\left(\frac{\pi}{\delta/mc}(u_n - u_0) \right) \right]$$

$$A_0 = \frac{2\pi^2}{N_X} \frac{\omega}{c} \frac{\omega_p^2}{\omega^2} \left| 1 - \frac{i\varepsilon_{12}}{\varepsilon_{11}} \right|^2 \frac{\mu e^{-\mu}}{4\pi K_2(\mu)} \qquad A_n = \mu^{n-1} \frac{n\omega_c}{\omega} u_n^{2n} \left(\frac{N_X \omega}{\sqrt{\mu}\omega_c} \right)^{2(n-1)} \frac{B(n+1, 1/2)}{[2^n(n-1)!]^2}$$

$$\mu = \frac{mc^2}{T_e} \qquad u_n = \left[\left(\frac{n\omega_c}{\omega} \right)^2 - 1 \right]^{1/2} \qquad u_0 = \frac{p_0}{mc} \qquad h(u_n) = H\left(u_n - u_0 + \frac{\delta}{mc} \right) H\left(u_0 + \frac{\delta}{mc} - u_n \right)$$

N_X , ε_{11} , ε_{12} → cold plasma X-mode refractive index and dielectric tensor elements

$B(x, y)$ = Beta function $K_2(x)$ = modified Bessel function $H(x)$ = Heaviside function

$$\boldsymbol{\beta} = \boldsymbol{A_0} \sum_{\boldsymbol{n}} \boldsymbol{\beta_n} \qquad \beta_n = A_n \frac{mc^2 u_n}{n\omega_c/\omega} \left[e^{-\mu\left(\frac{n\omega_c}{\omega}-1\right)} + Q_n h(u_n) f_0 sin\left(\frac{\pi}{\delta/mc}(u_n - u_0) \right) \right]$$

$$f_1 = f_{1u} \rightarrow Q_n = 1 \qquad f_1 = f_{1u} sin\theta \rightarrow Q_n = \frac{B(n+3/2, 1/2)}{B(n+1, 1/2)} \qquad f_1 = f_{1u} cos^2\theta \rightarrow Q_n = \frac{B(n+1, 3/2)}{B(n+1, 1/2)}$$

$$f_1 = f_{1u} sin^2(2\theta) \rightarrow Q_n = 4\frac{B(n+2, 3/2)}{B(n+1, 1/2)} \qquad f_1 = f_{1u} cos\theta \rightarrow Q_n = \frac{B(n+1, 1)}{B(n+1, 1/2)}$$

ECE X2 profiles affected at high temperature only

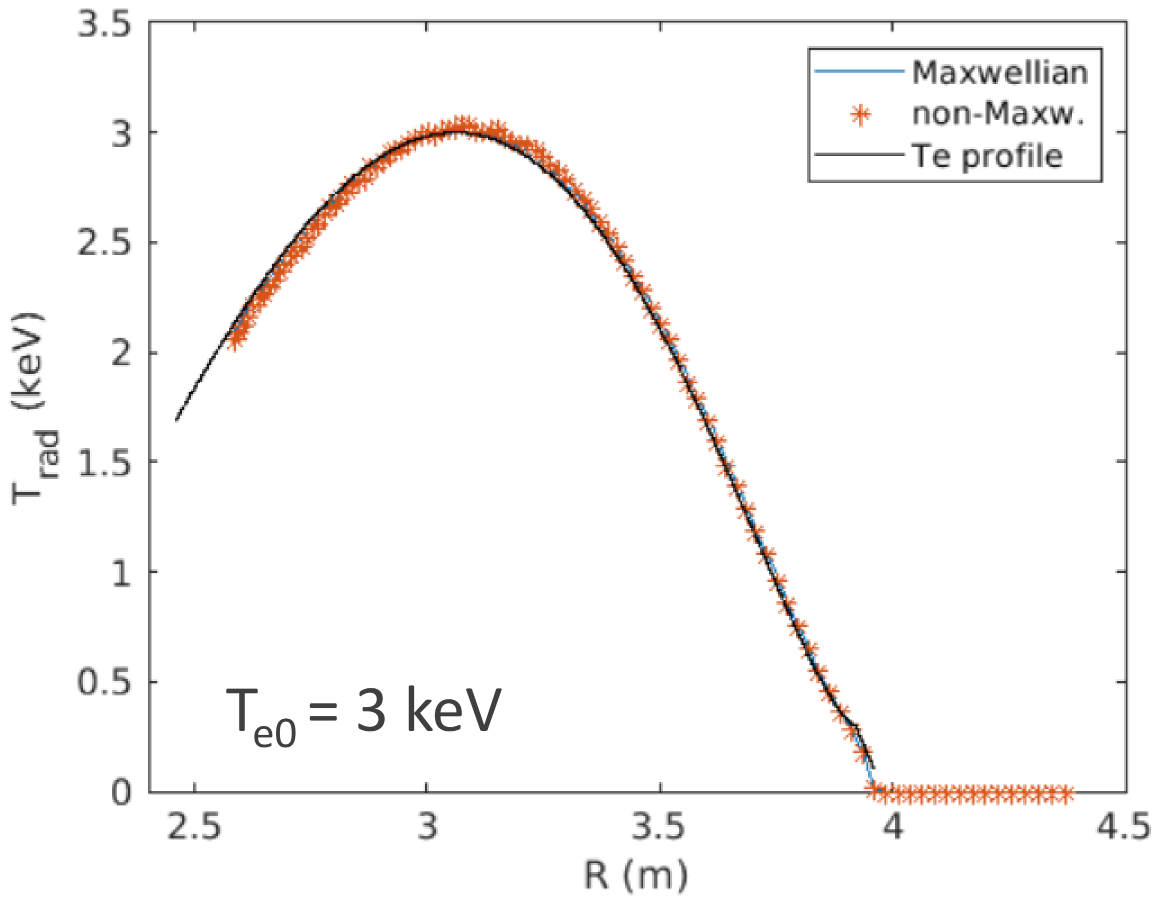

isotropic perturbation, $f_0 = 0.03$ $p_0/p_{th} = 1$ $\delta/p_{th} = 0.25$

ECE X2 profiles affected at high temperature only

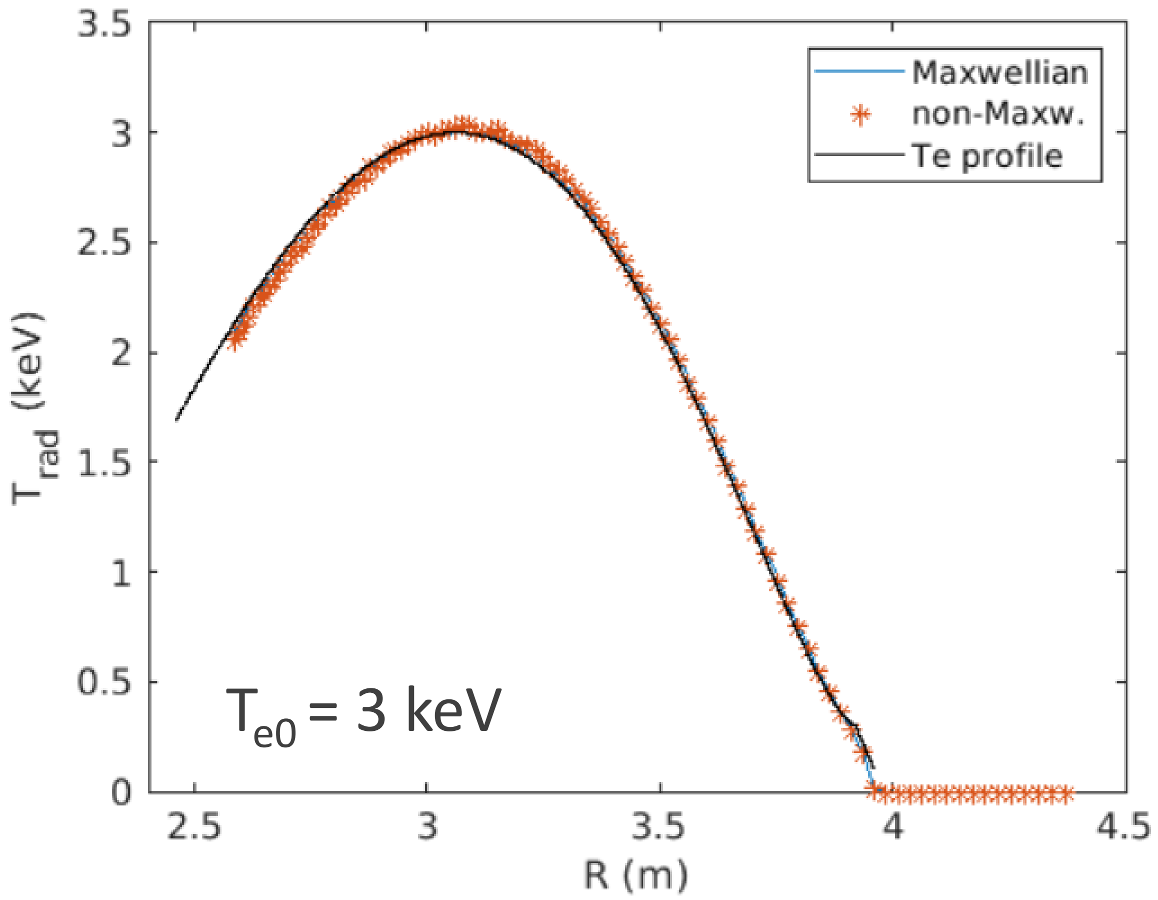

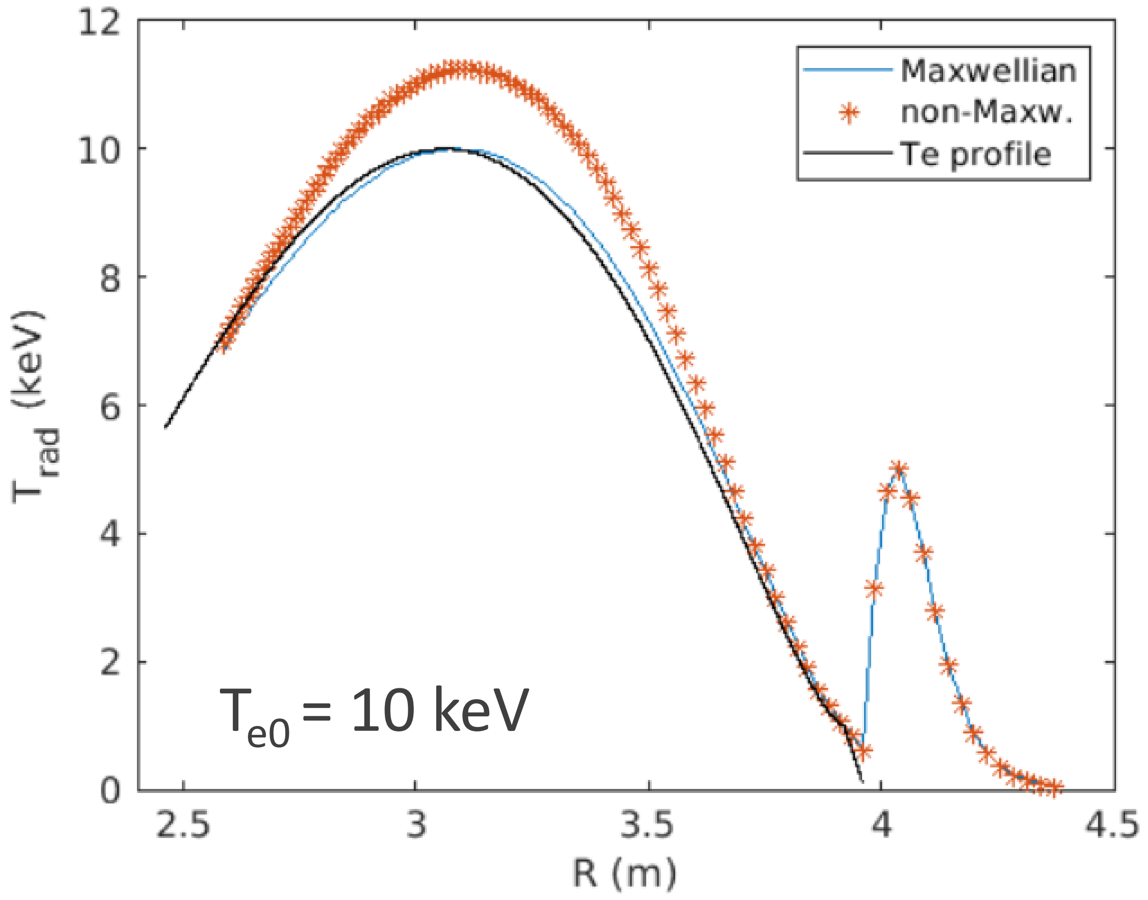

isotropic perturbation, $f_0 = 0.03$ $p_0/p_{th} = 1$ $\delta/p_{th} = 0.25$

Effect of perturbation on ECE X2 and Thomson spectra

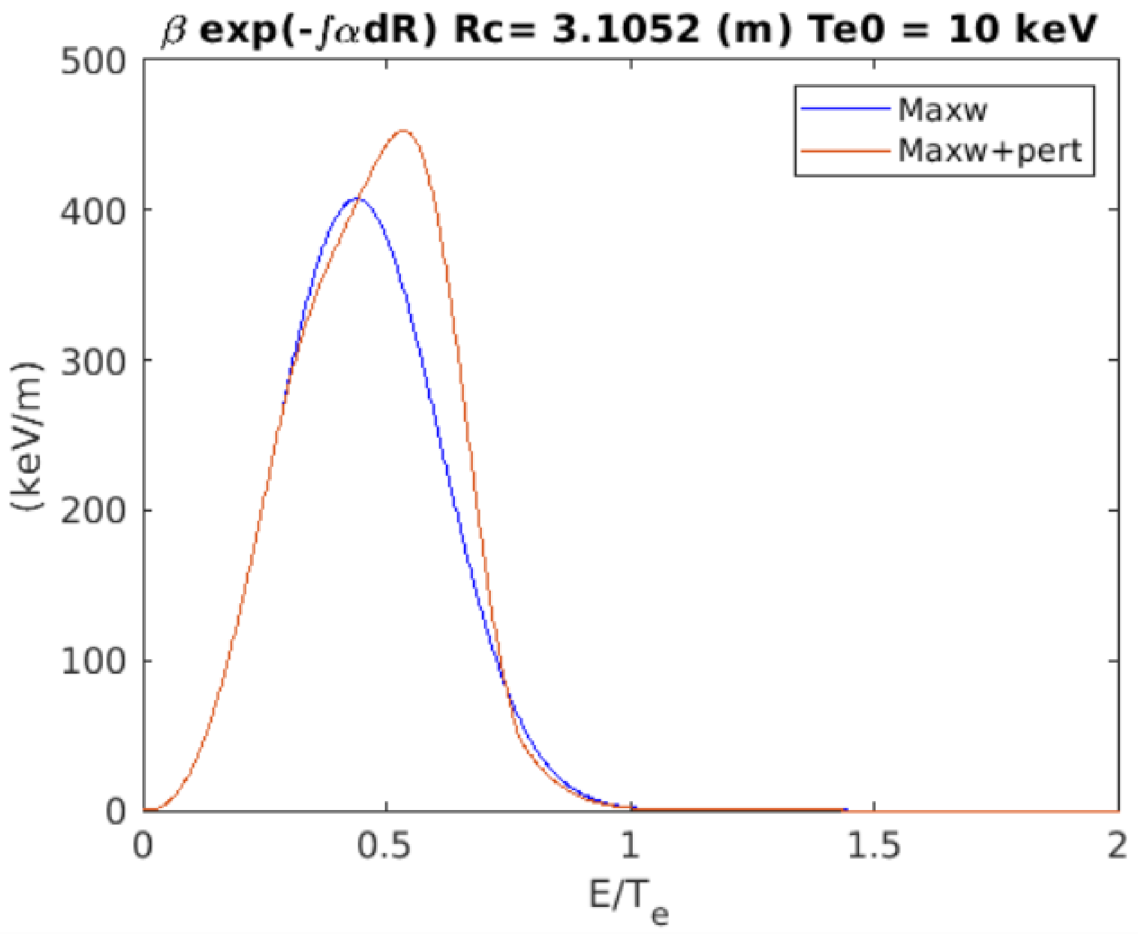

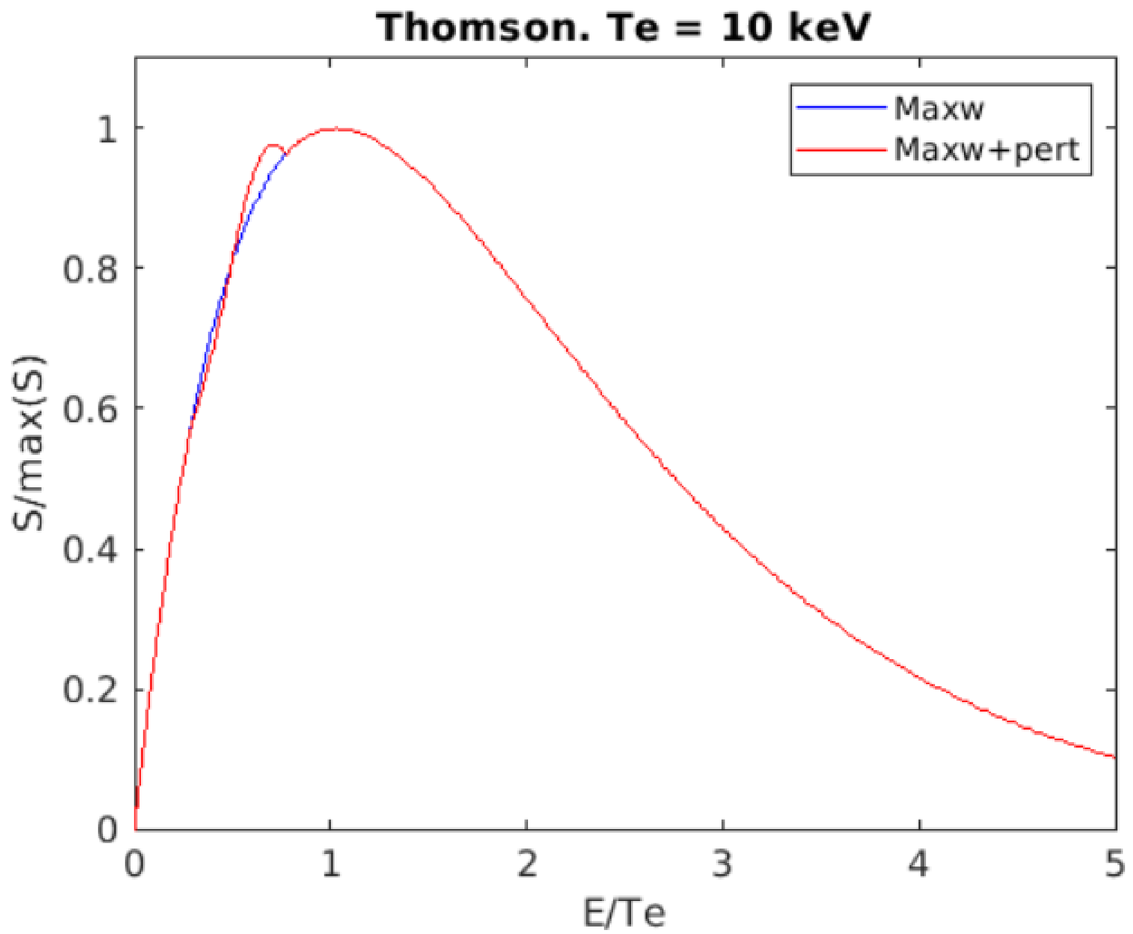

DD baseline database *"with low gas+pellets+small Neon injection"*

96990, 96992, 96993, 96994, 96996, 96998, 96999

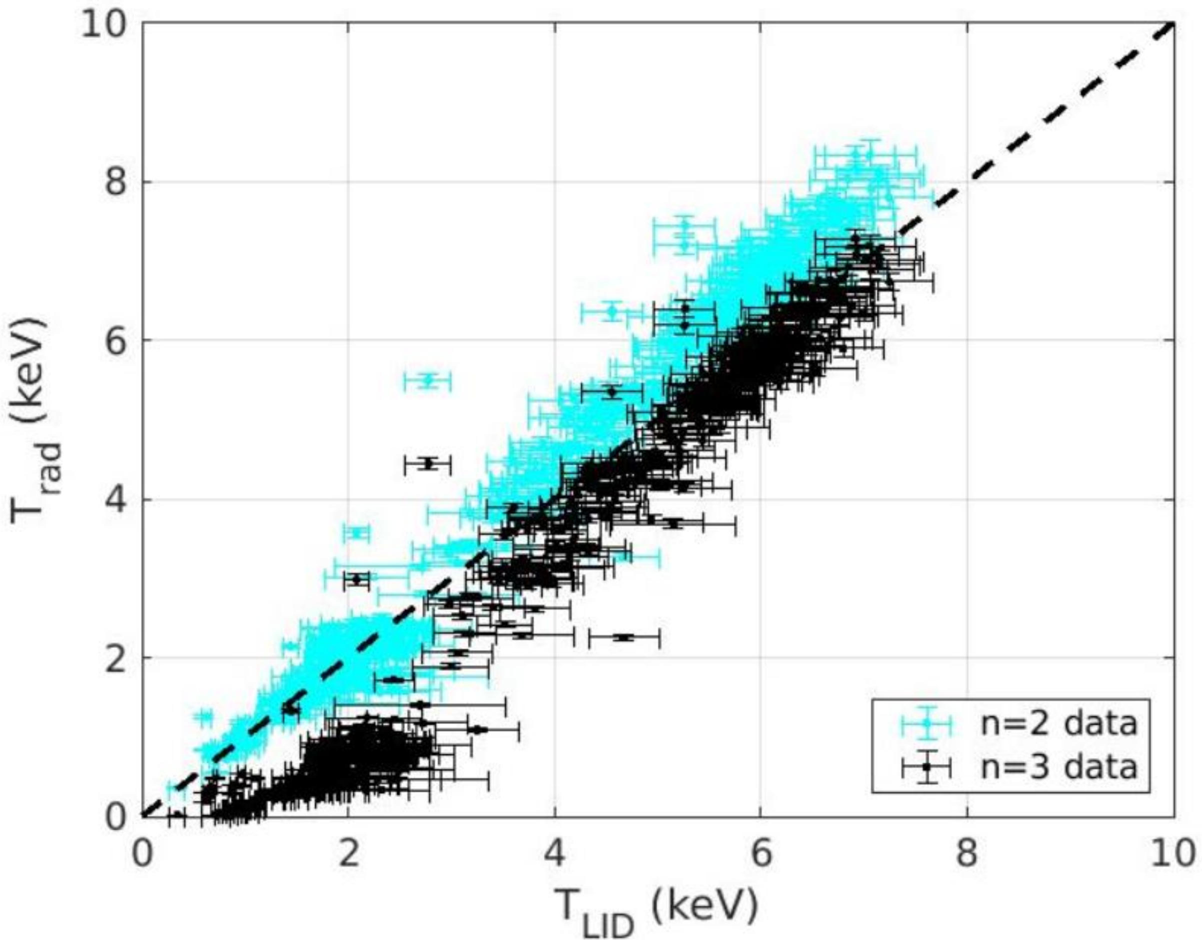

J. Garcia et al Phys. Plasmas **29**, 032505 (2022)

DD baseline database *"with low gas+pellets+small Neon injection"*

96990, 96992, 96993, 96994, 96996, 96998, 96999

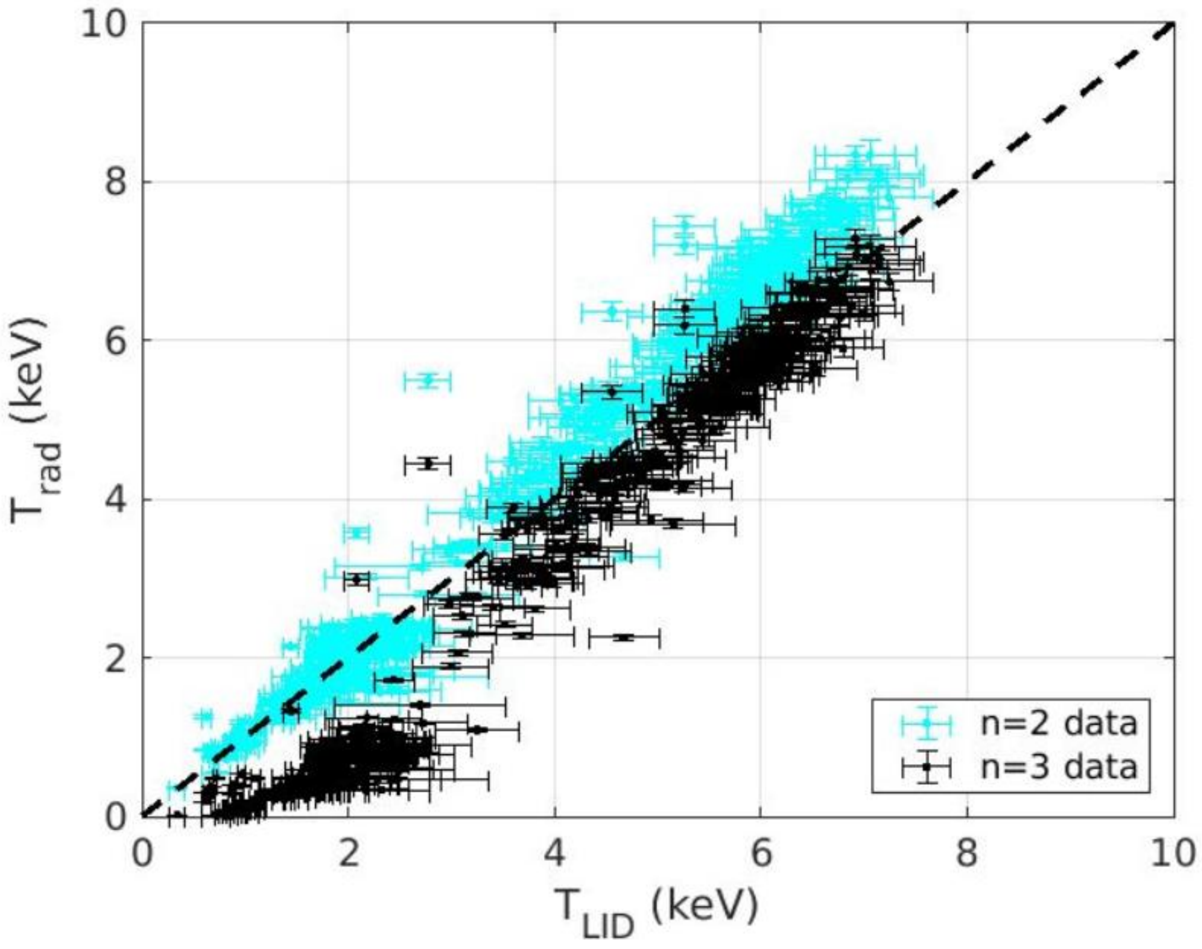

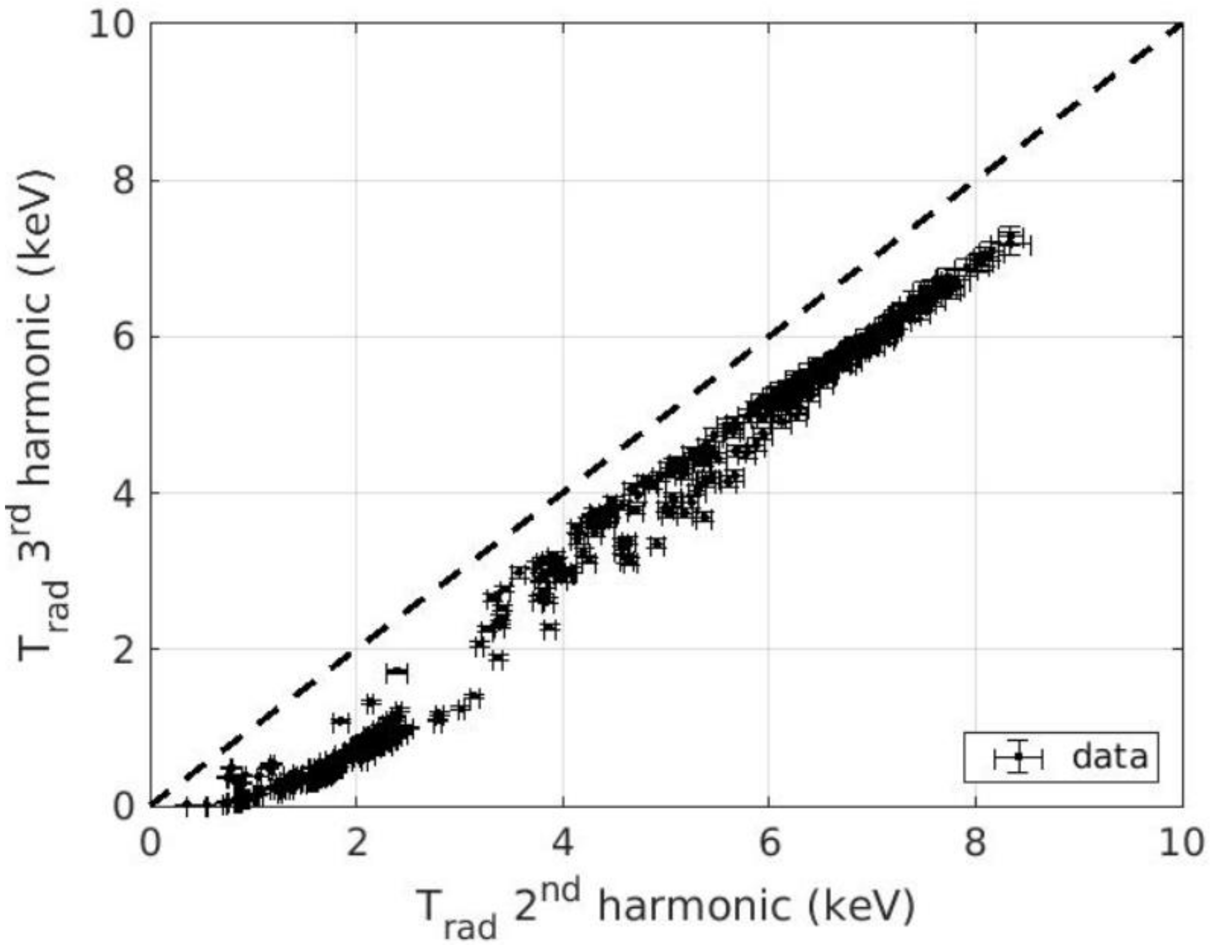

J. Garcia et al Phys. Plasmas **29**, 032505 (2022)

DD baseline database *"with low gas+pellets+small Neon injection"*

96990, 96992, 96993, 96994, 96996, 96998, 96999

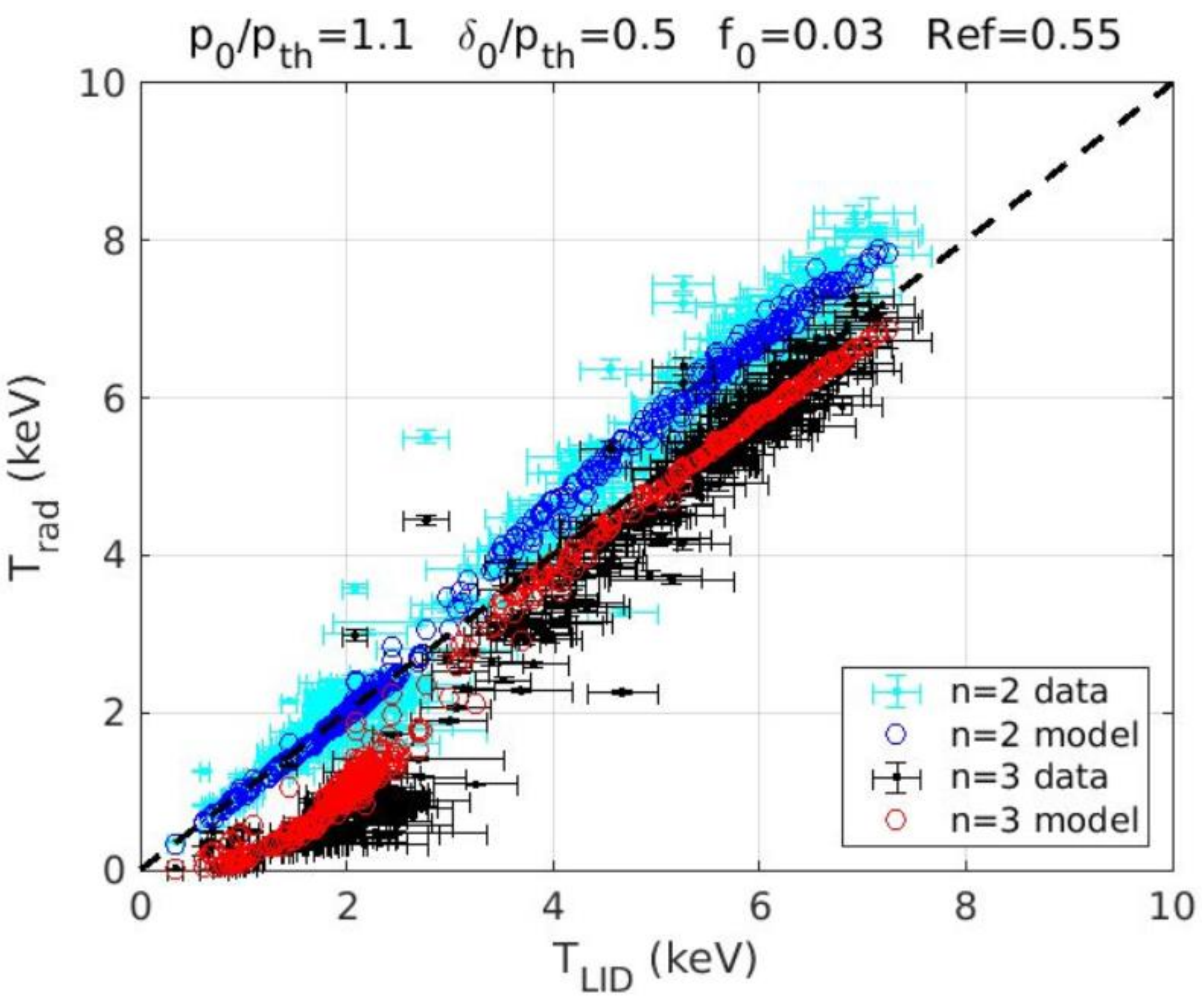

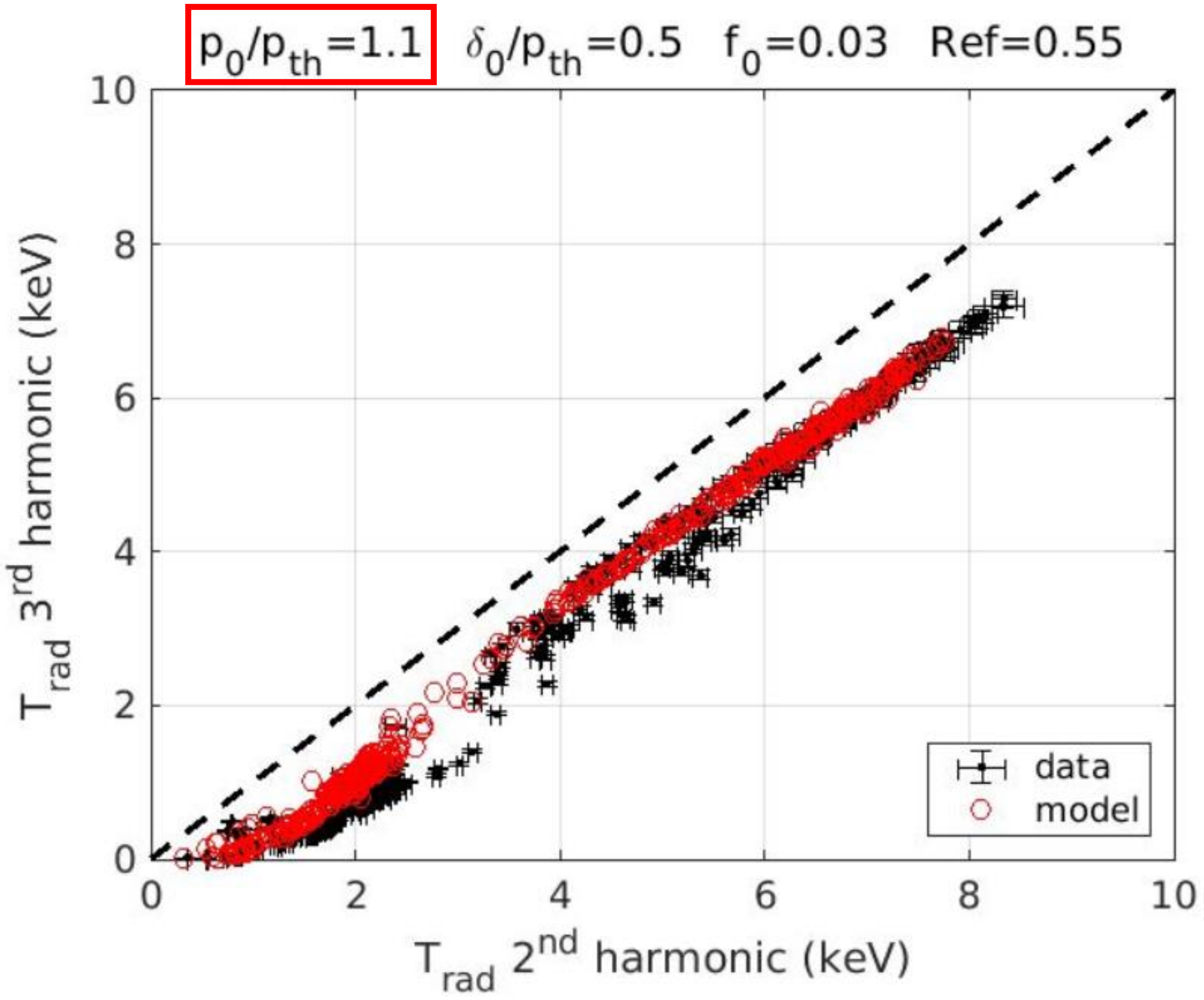

J. Garcia et al Phys. Plasmas **29**, 032505 (2022)

DT baseline database

99520, 99795, 99796, 99797, 99799, 99805, 99861, 99862, 99863, 99878, 99943, 99944, 99948

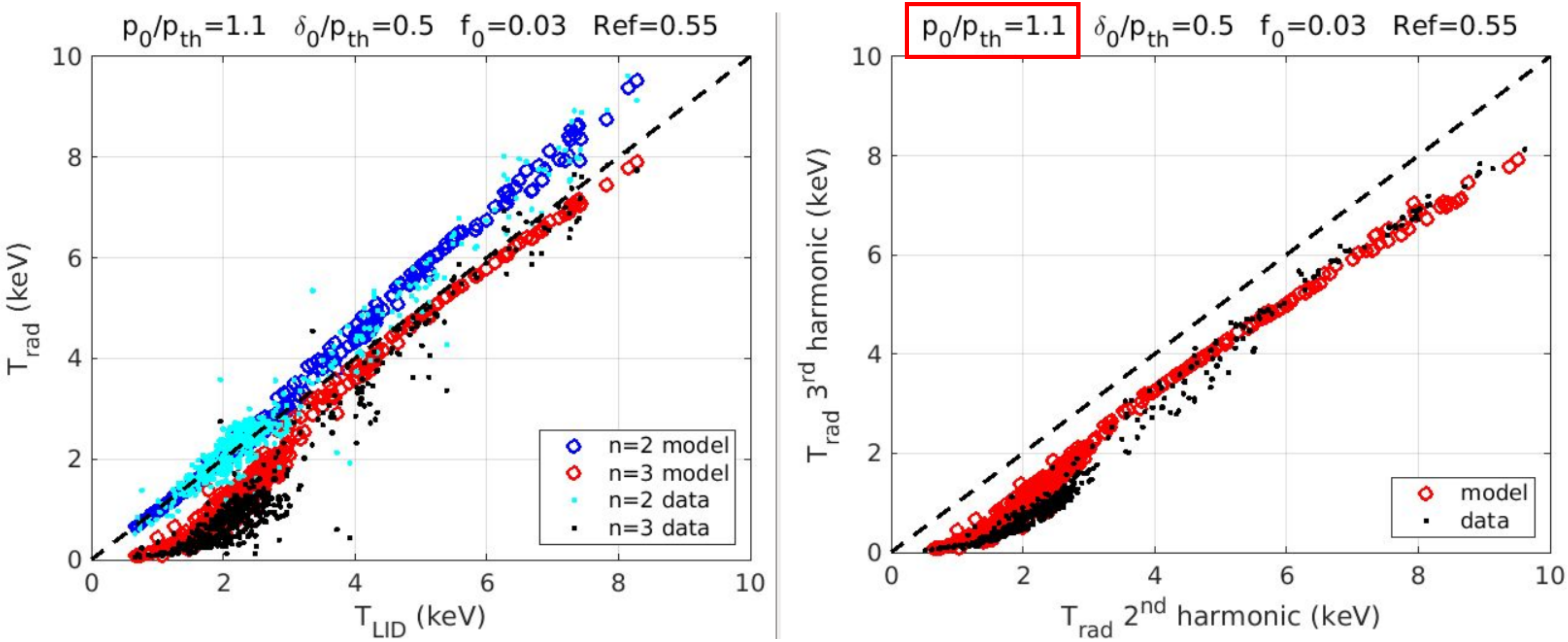

DT hybrid database

99448, 99449, 99450, 99452, 99455, 99541, 99542, 99543, 99544, 99594, 99595, 99596, 99760, 99761, 99866, 99867, 99868, 99869, 99908, 99910, 99912, 99914, 99949, 99950, 99951, 99953

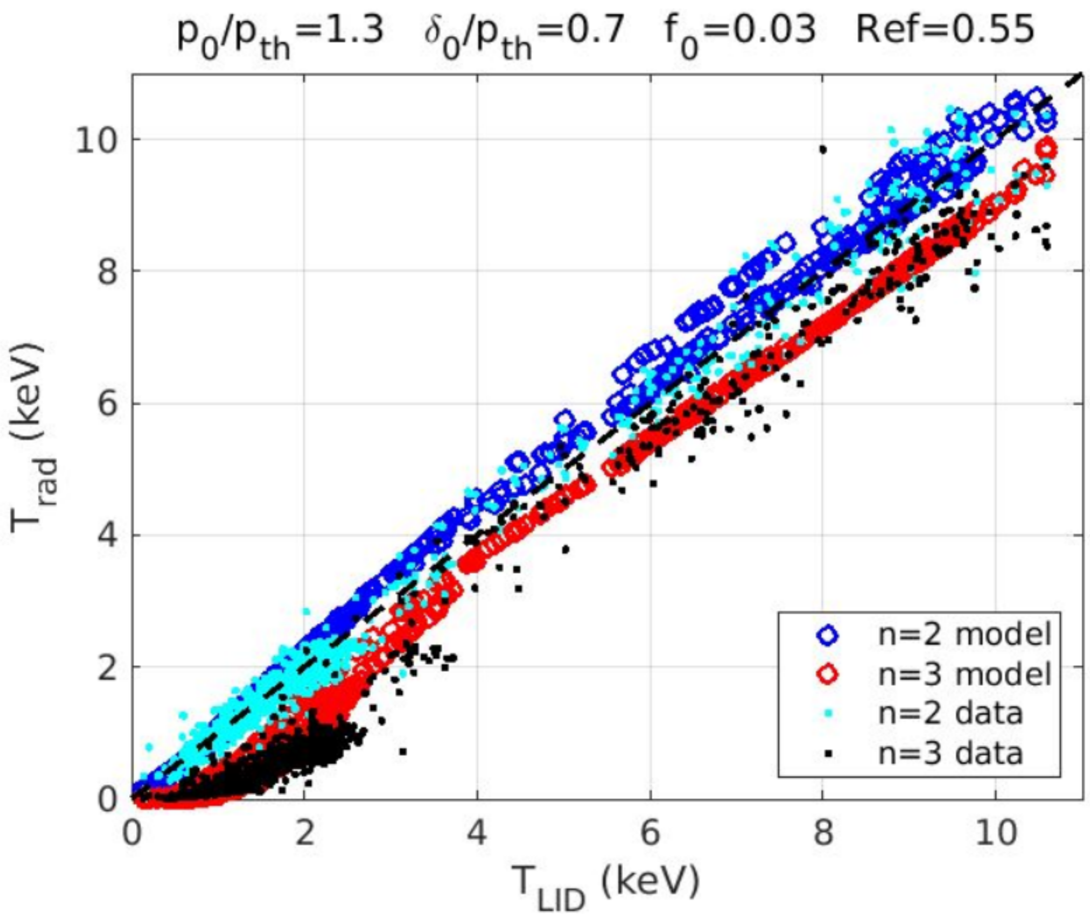

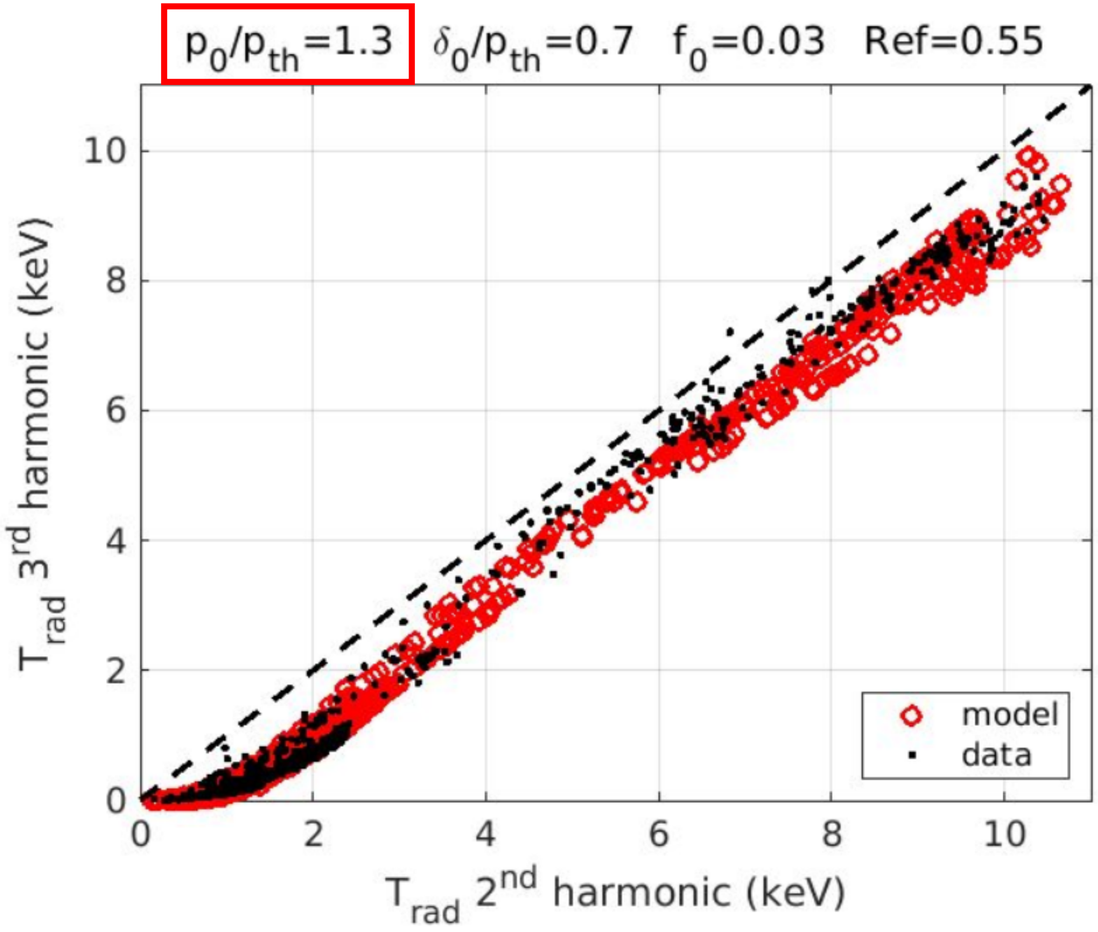

DD M18-03 experiment, pulse 96850

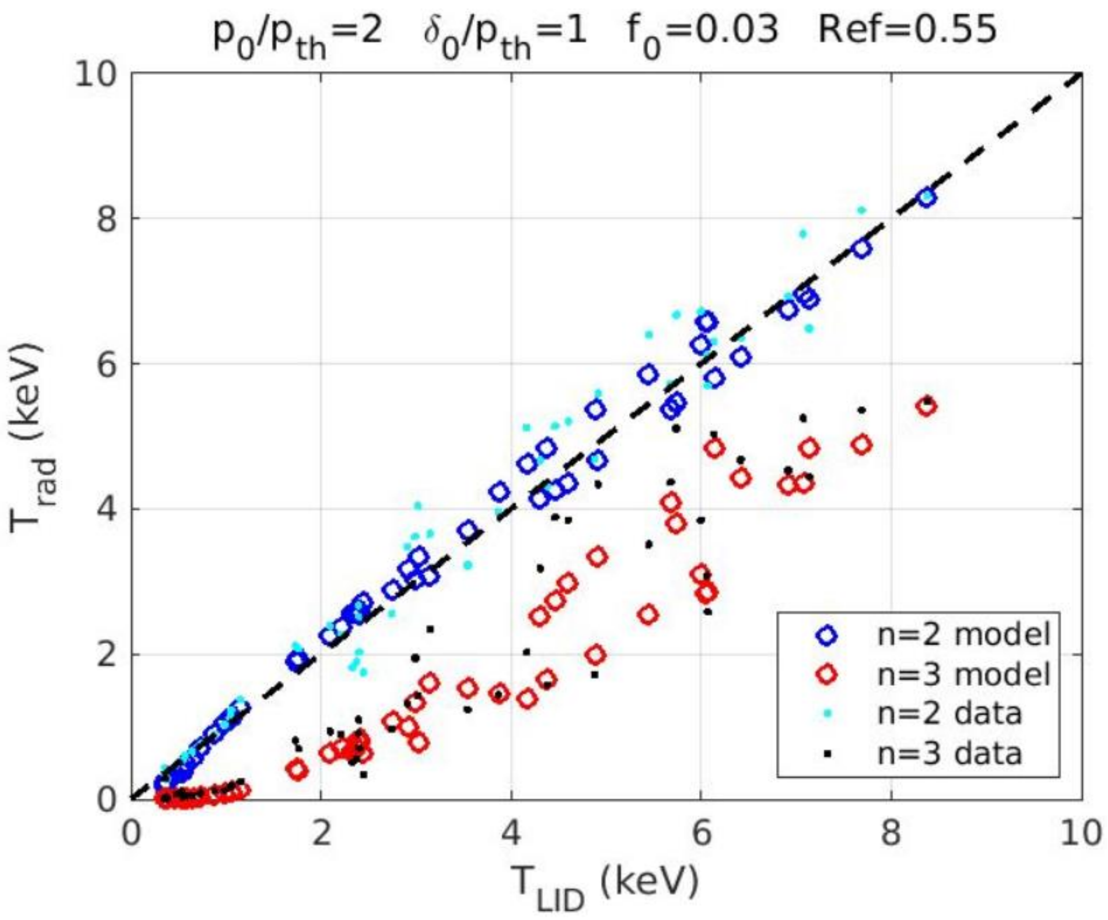

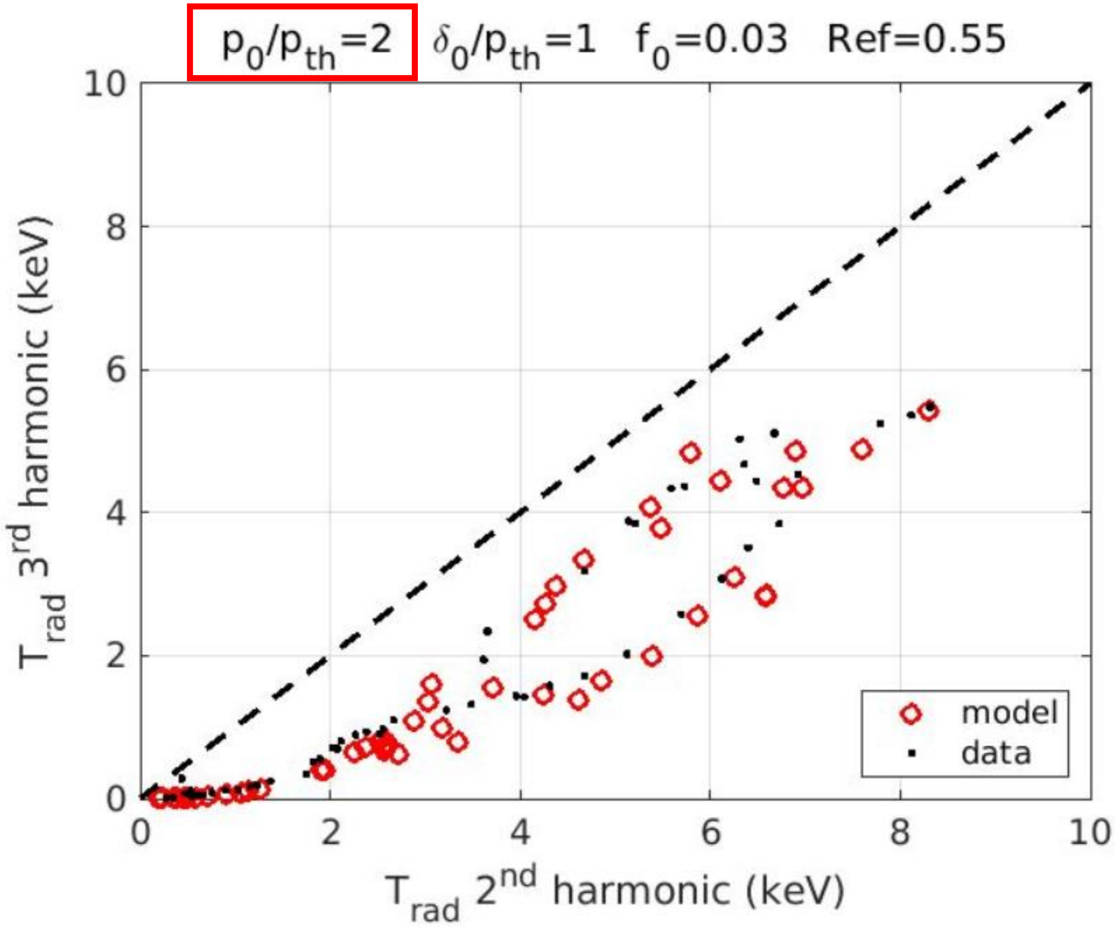

Scenario for specific studies on Energetic Particles.
Low density (< 5 10^{19} m^{-3}). High temperature phase with ICRH only

ITER: two cases with different perturbations

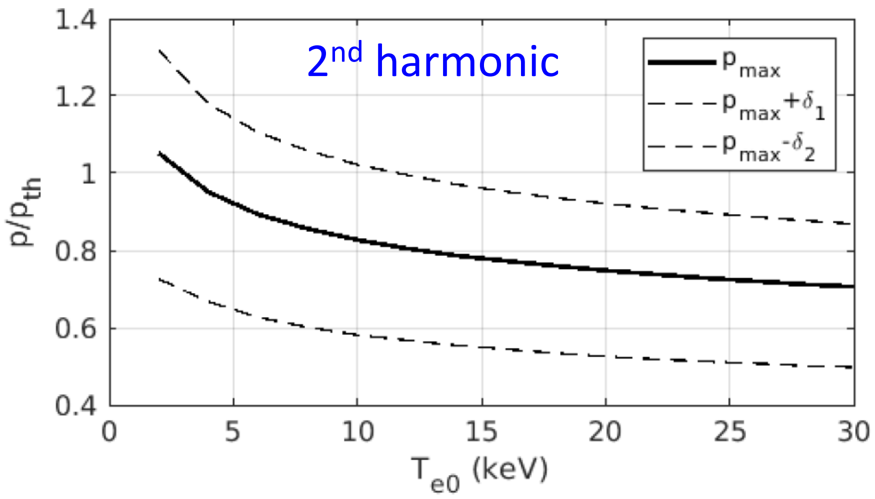

ITER: two cases with different perturbations

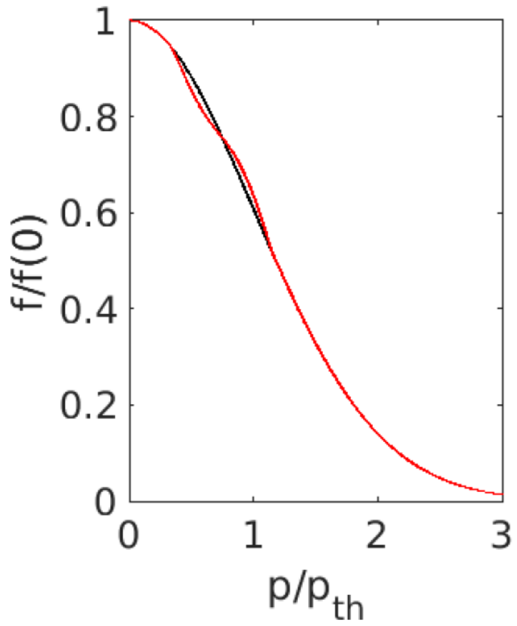

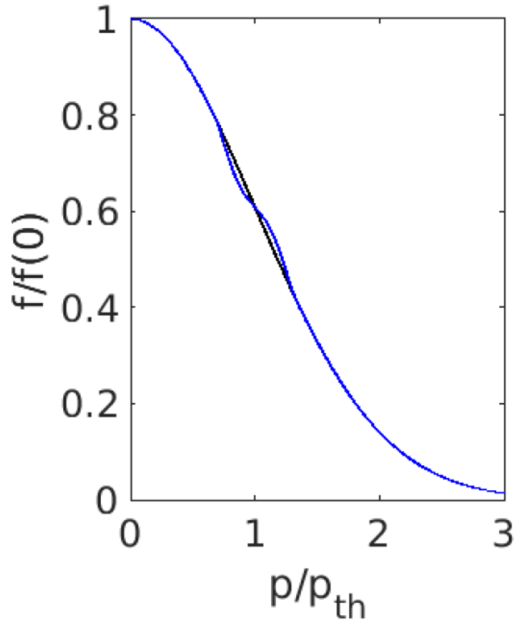

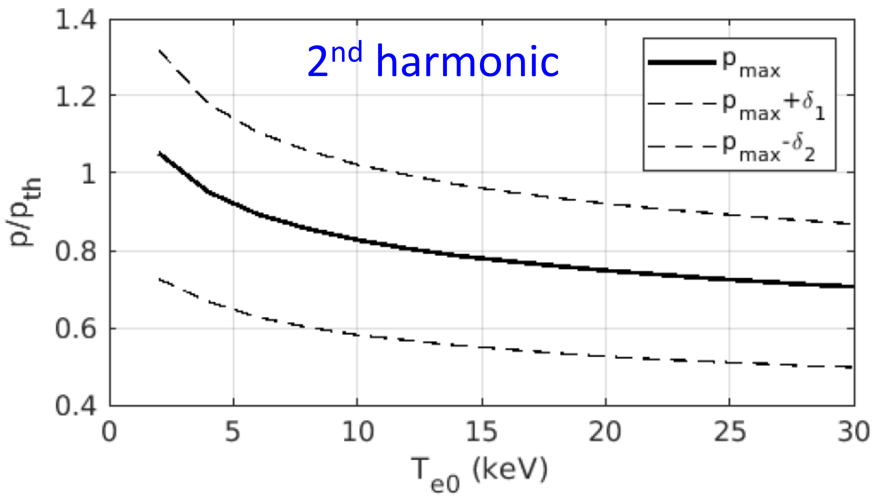

ITER: two cases with different perturbations

2nd harmonic

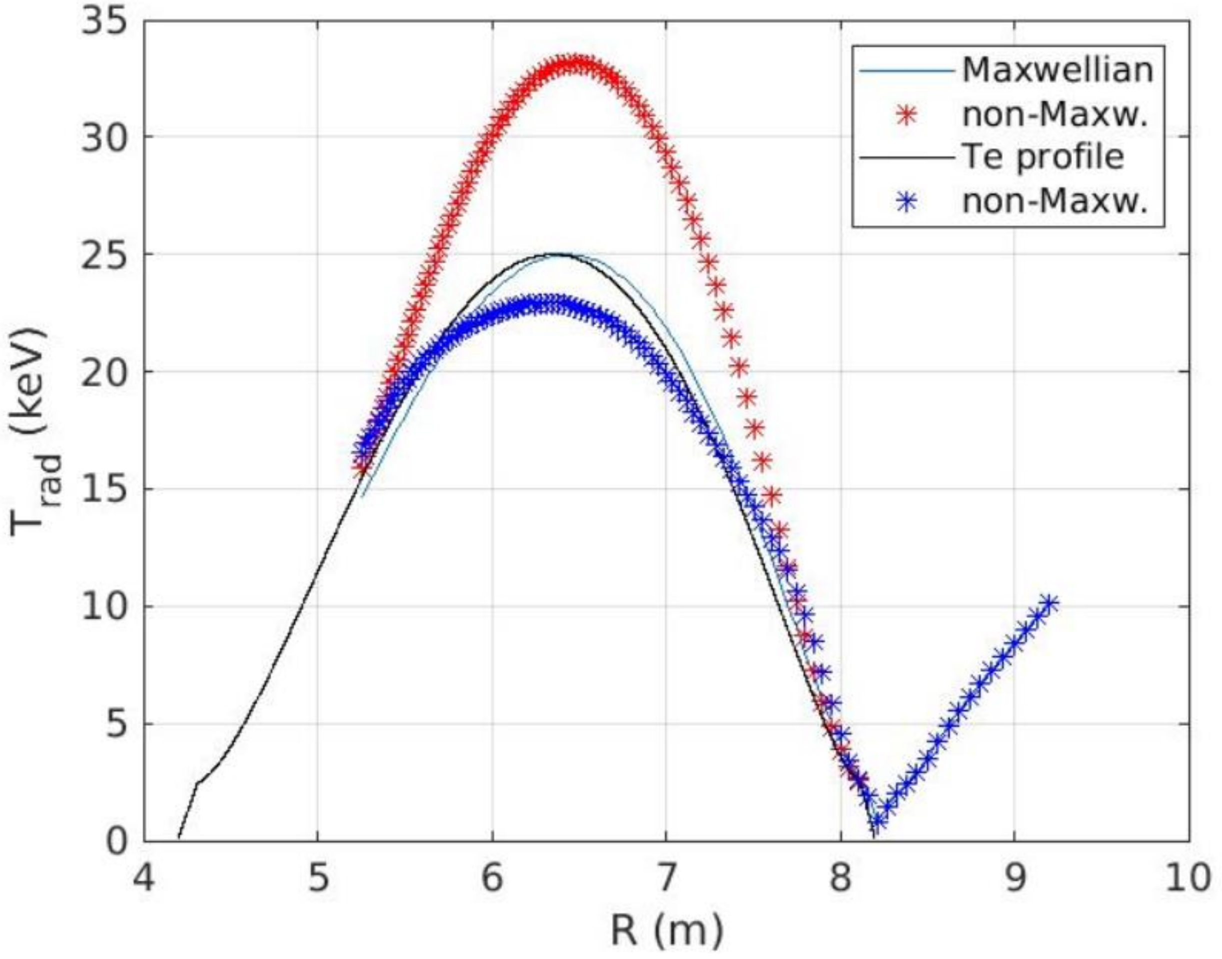

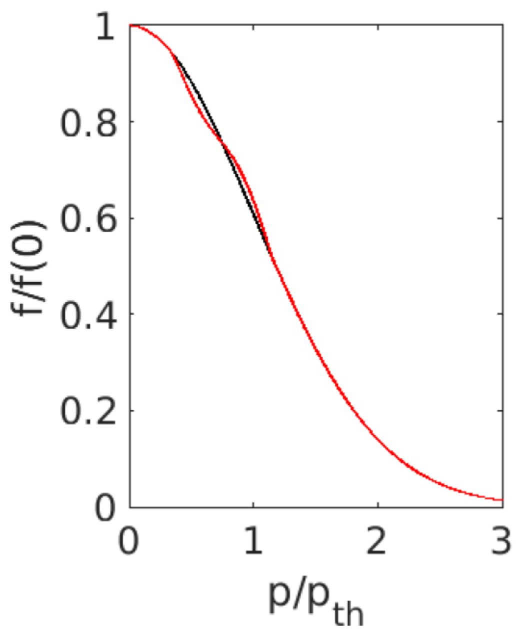

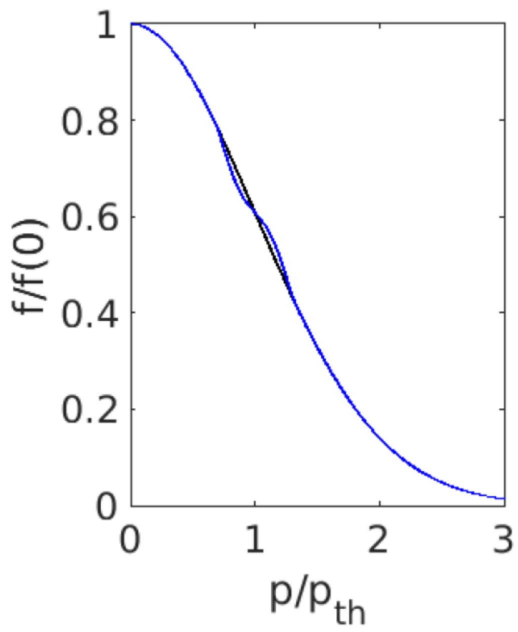

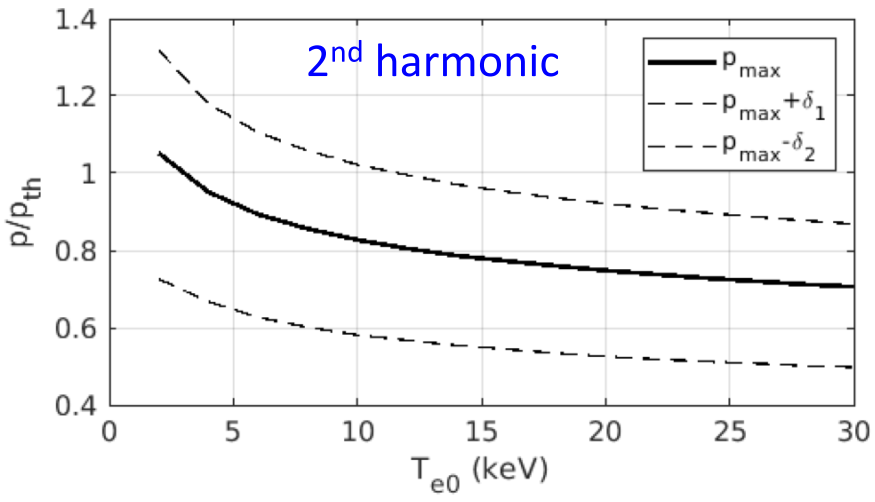

Conclusions

- **Using the model of perturbed electron distribution we have shown that :**
  - a perturbation of < 5% yields the expected effect at T_e ~ 5-10 keV (ΔT_{rad} ~1 keV)
  - even if present, the perturbation cannot be observed at low temperature
  - Thomson spectrum is broad and insensitive to such perturbations

- **Consequences :**
  - In principle, Thomson scattering seems more reliable for T_e measurements at high temperature
  - ECE is very effective for constraining the distribution function → tool to explore new physics

- **Origin of the effect is under investigation. Two possible causes :**
  - fast ion collisional relaxation on electrons → needs full kinetic calculation with integro-differential collision operator → work in progress (R. Dumont)
  - Landau damping of fast ion driven (or other high-β) MHD modes
    - bipolar electron distributions observed in the magnetosheath → *C.H.K. Chen et al., Nat. Commun. 10, 740 (2019)*
    - interpretation as Landau damping of Kinetic Alfvén Waves confirmed by gyrokinetic simulations → *S.A. Horvath et al., Phys. Plasmas 27, 102901 (2020)*
    - gyrokinetic modelling with GENE for JET parameters → work in progress (S. Mazzi)

Backup slides

What is seen by 2nd harmonic ECE (in space)

<u>In the following</u>:
analytic density and temperature profiles.
analytic equilibrium with Shafranov shift.

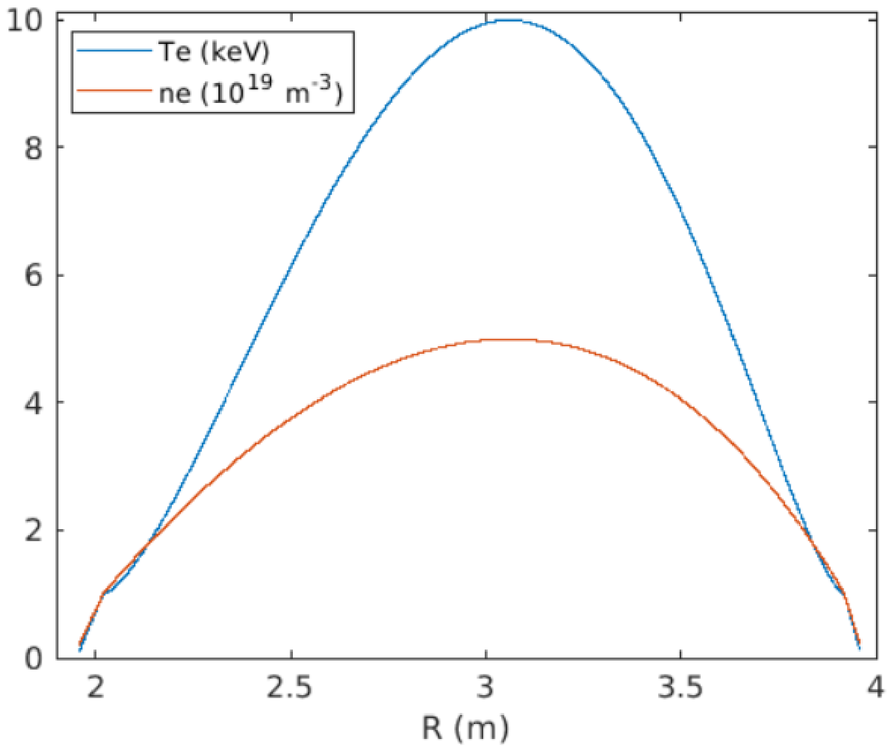

absorption/emission coefficients at different frequencies

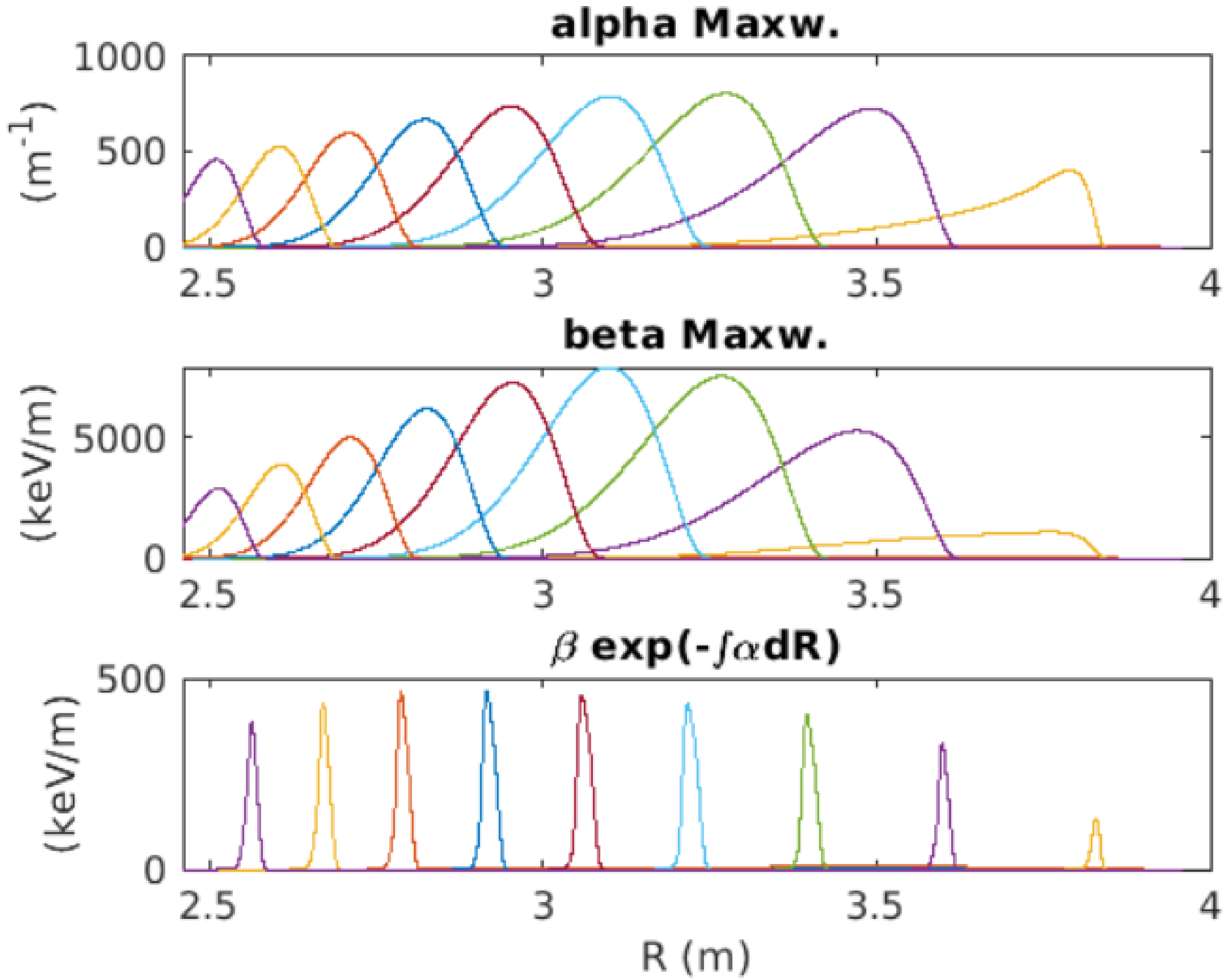

ECE sets constraints on the distribution function

$$f_M = Ae^{-E_k/T_e}$$

$$T_e = -\frac{f_M}{df_M/dE_k}$$

Note: here slopes are exaggerated

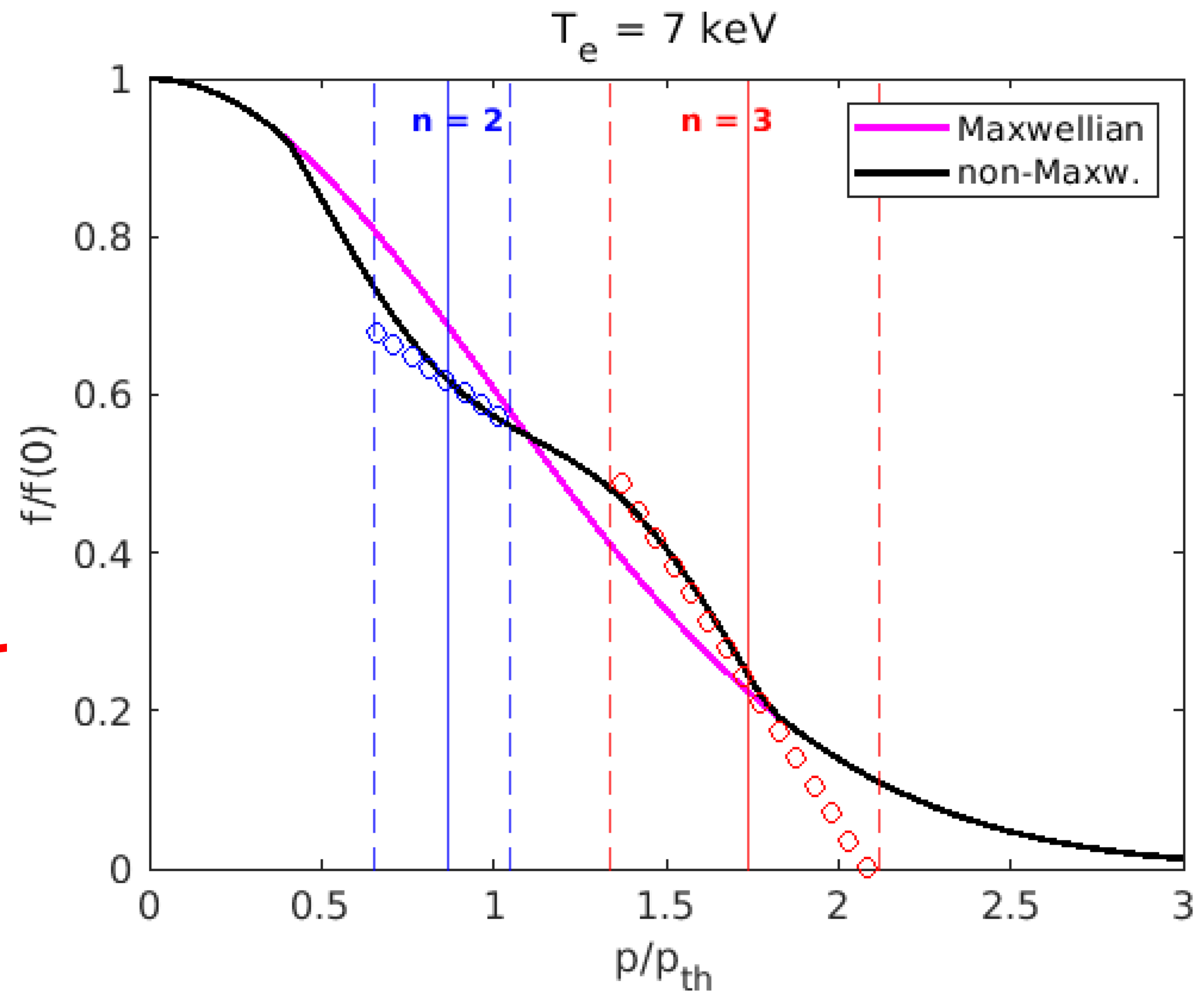

on average:

n=2 → $T_{rad} > T_e$

n=3 → $T_{rad} < T_e$

solid lines: maximum of $\beta \exp(-\int \alpha \, dR)$

dashed lines: width at half-heigth

Test of model perturbation on old data: one size fits all ?

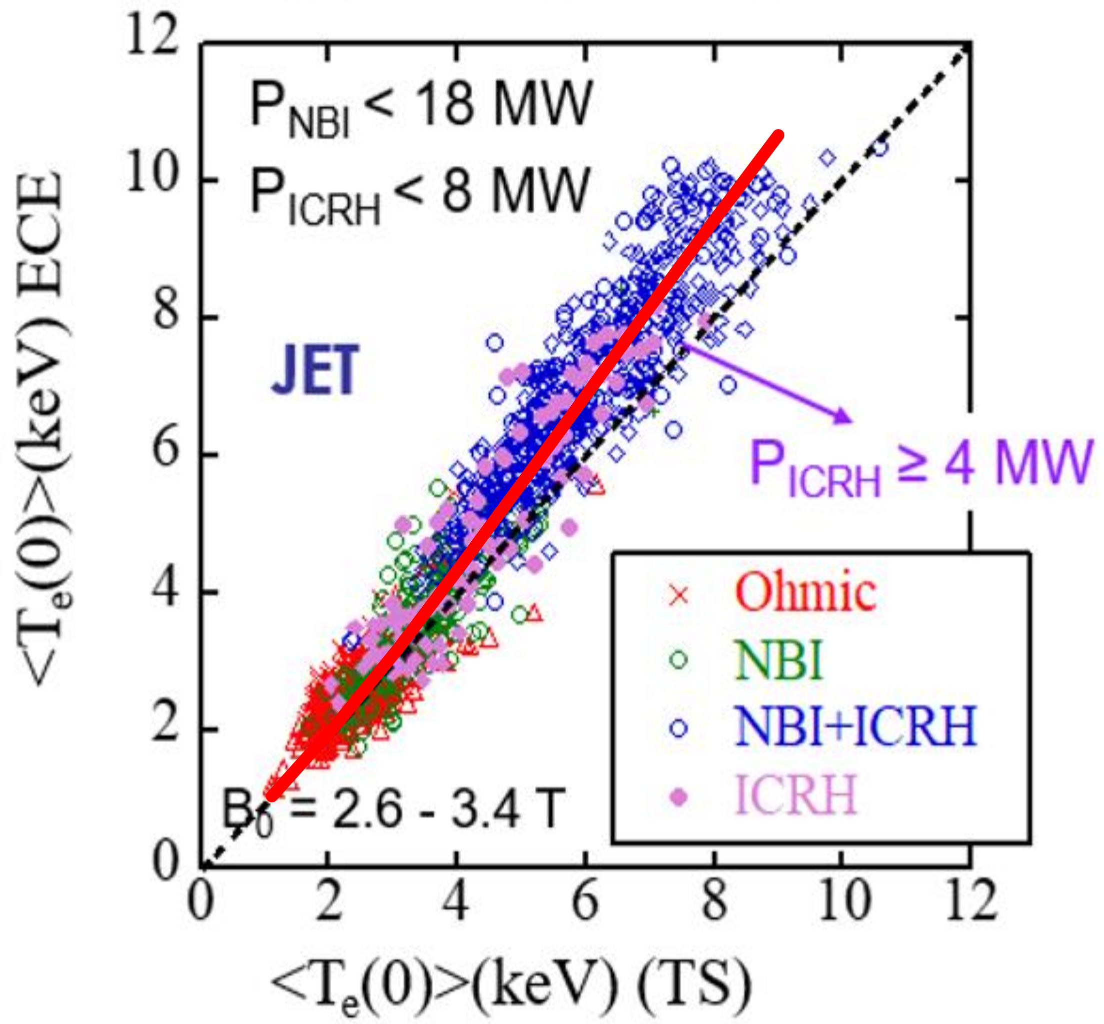

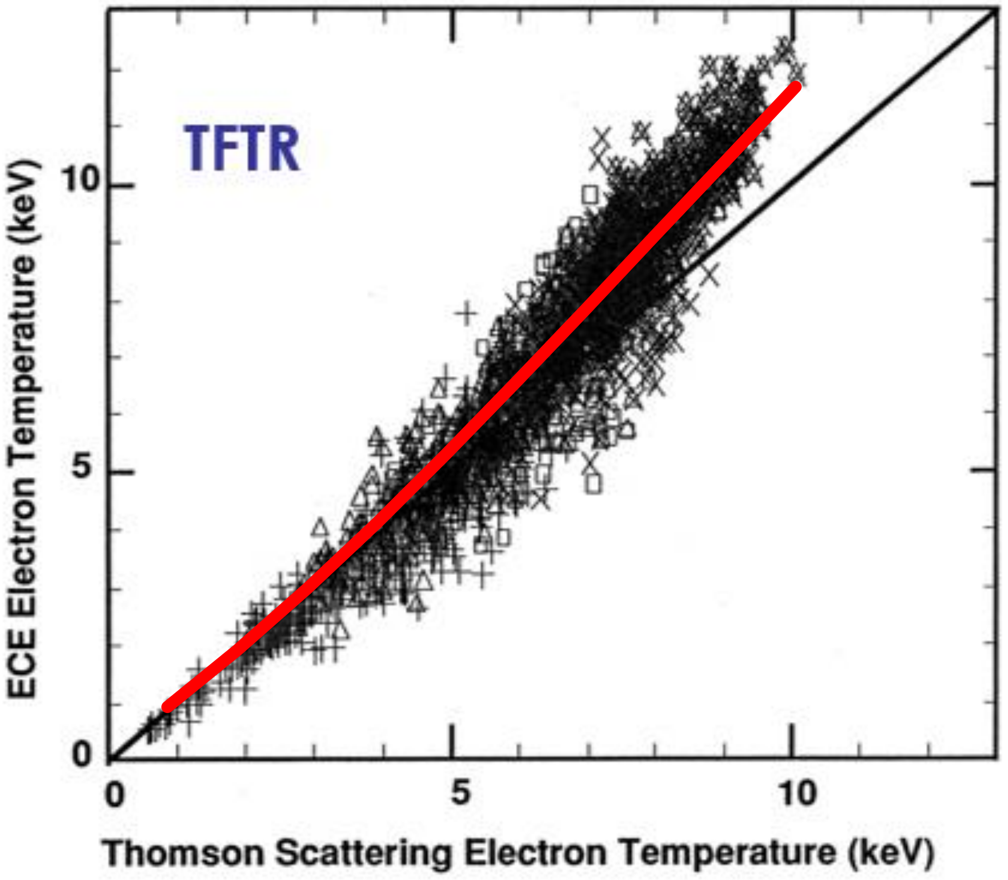

f_0 = 0.03
p_0/p_{th} = 1
δ/p_{th} = 0.4

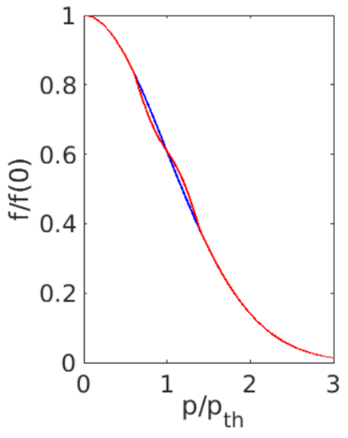

mean values of density and magnetic field used

All DT data points with NBI only

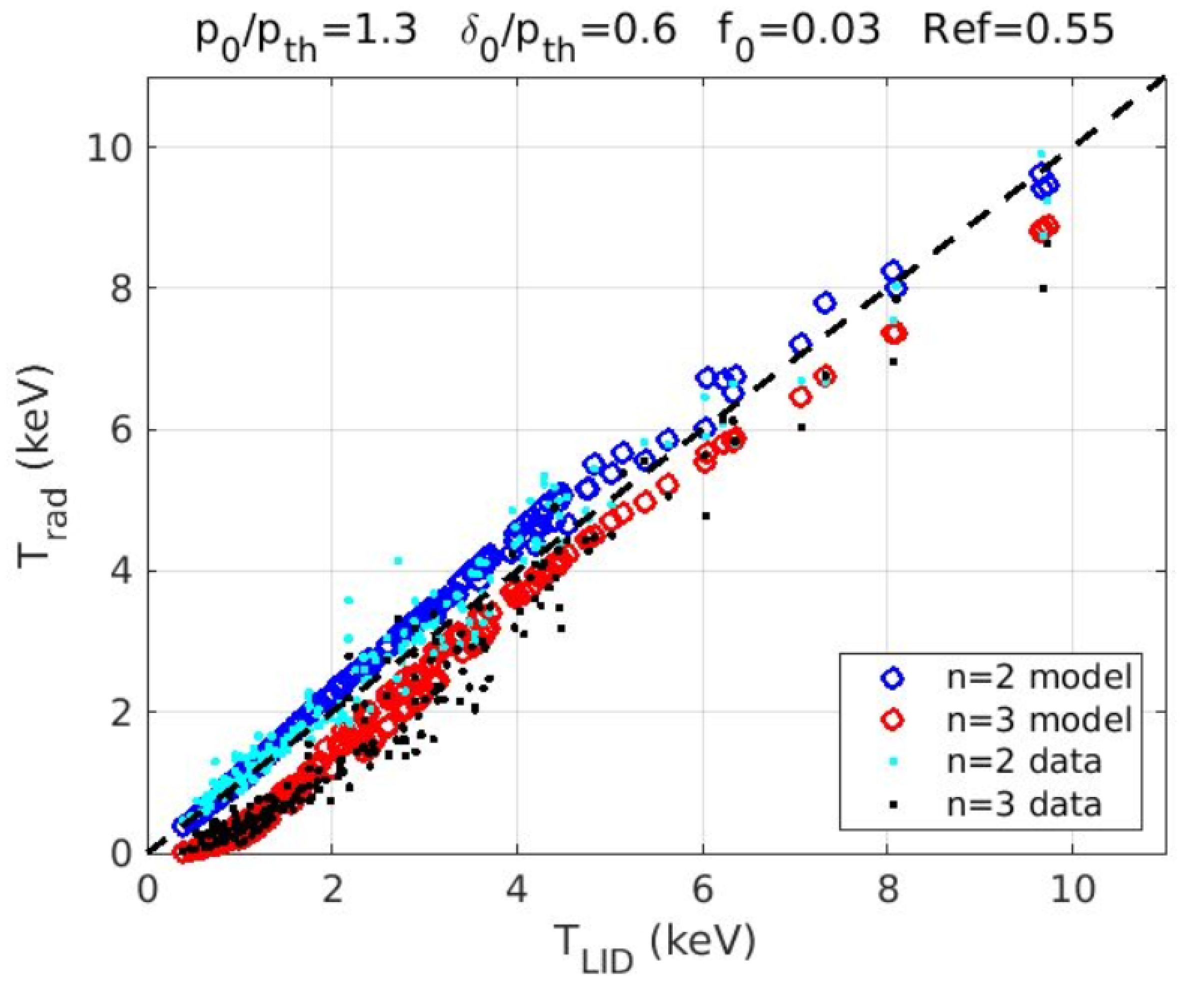

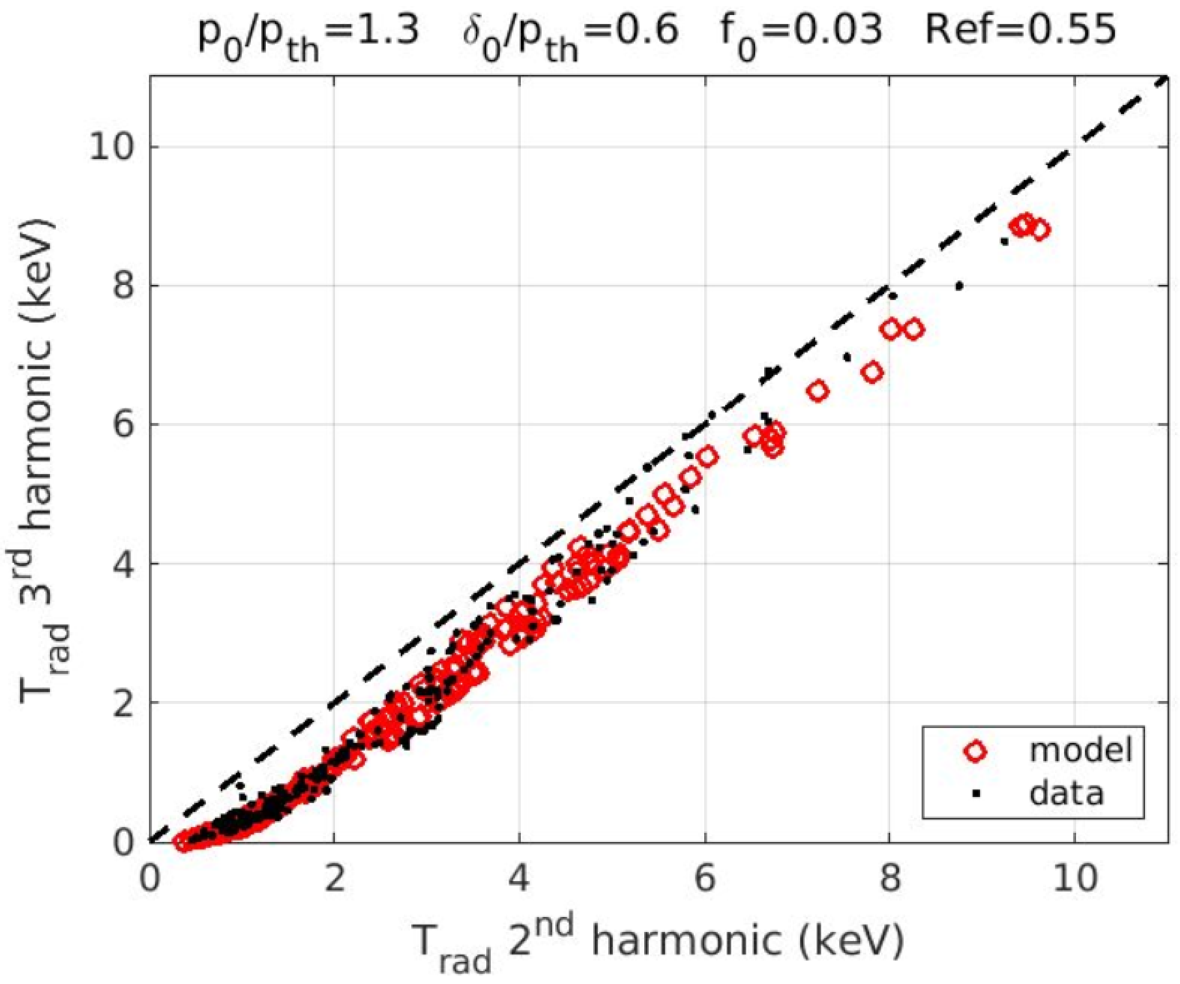

All DT data points with ICRH only

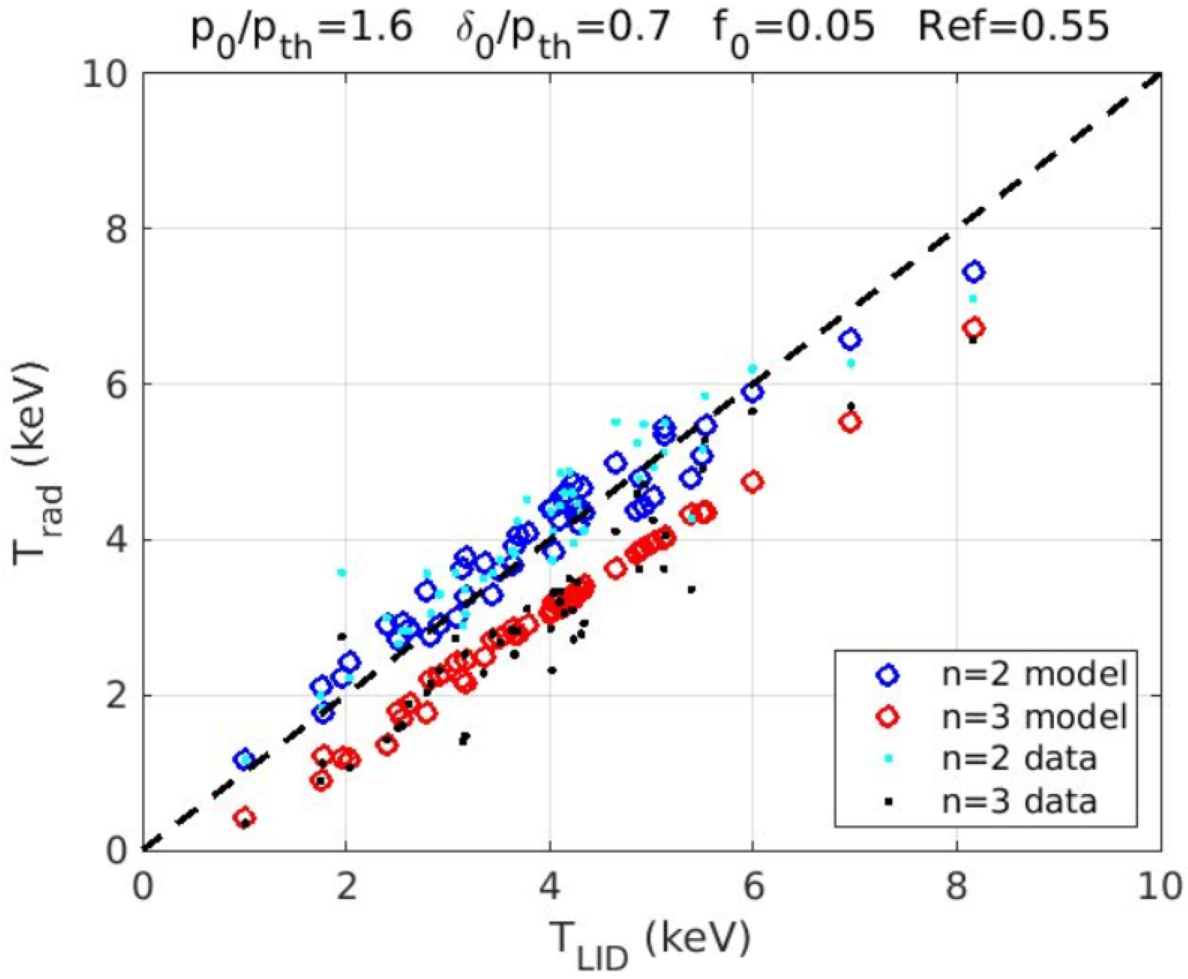

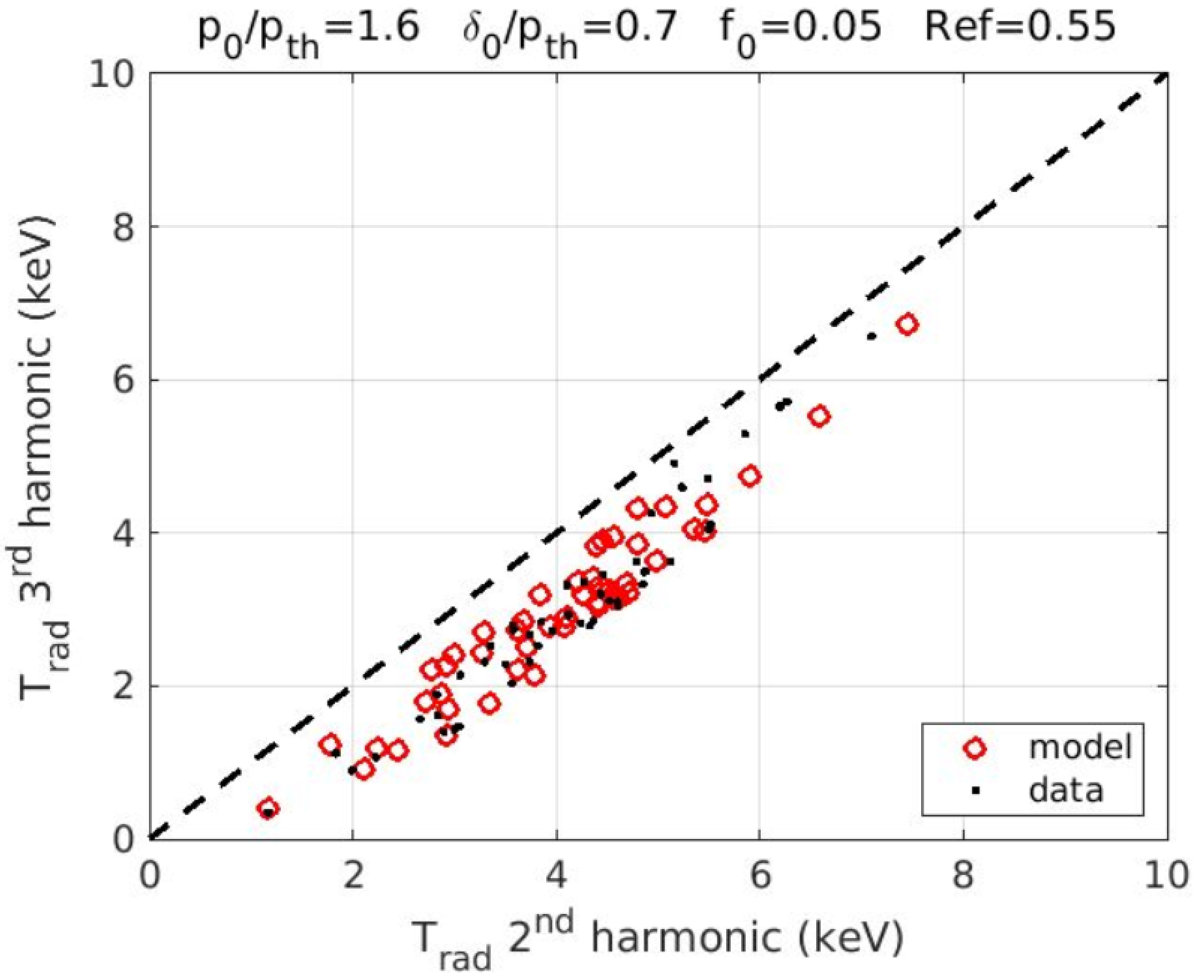

Perturbed electron distributions

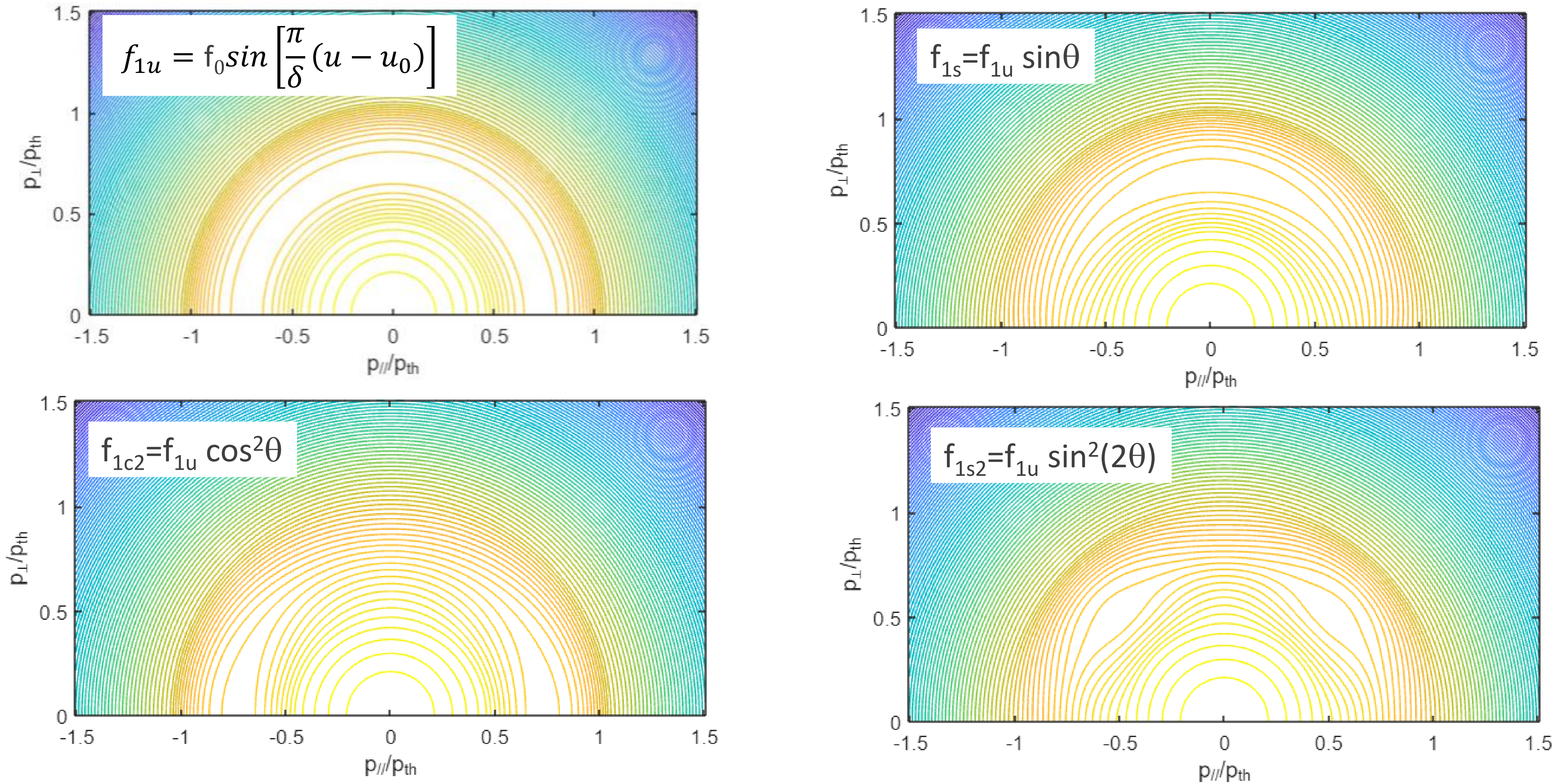

Use of the model for full database analysis: p_0/p_{th} as fit parameter

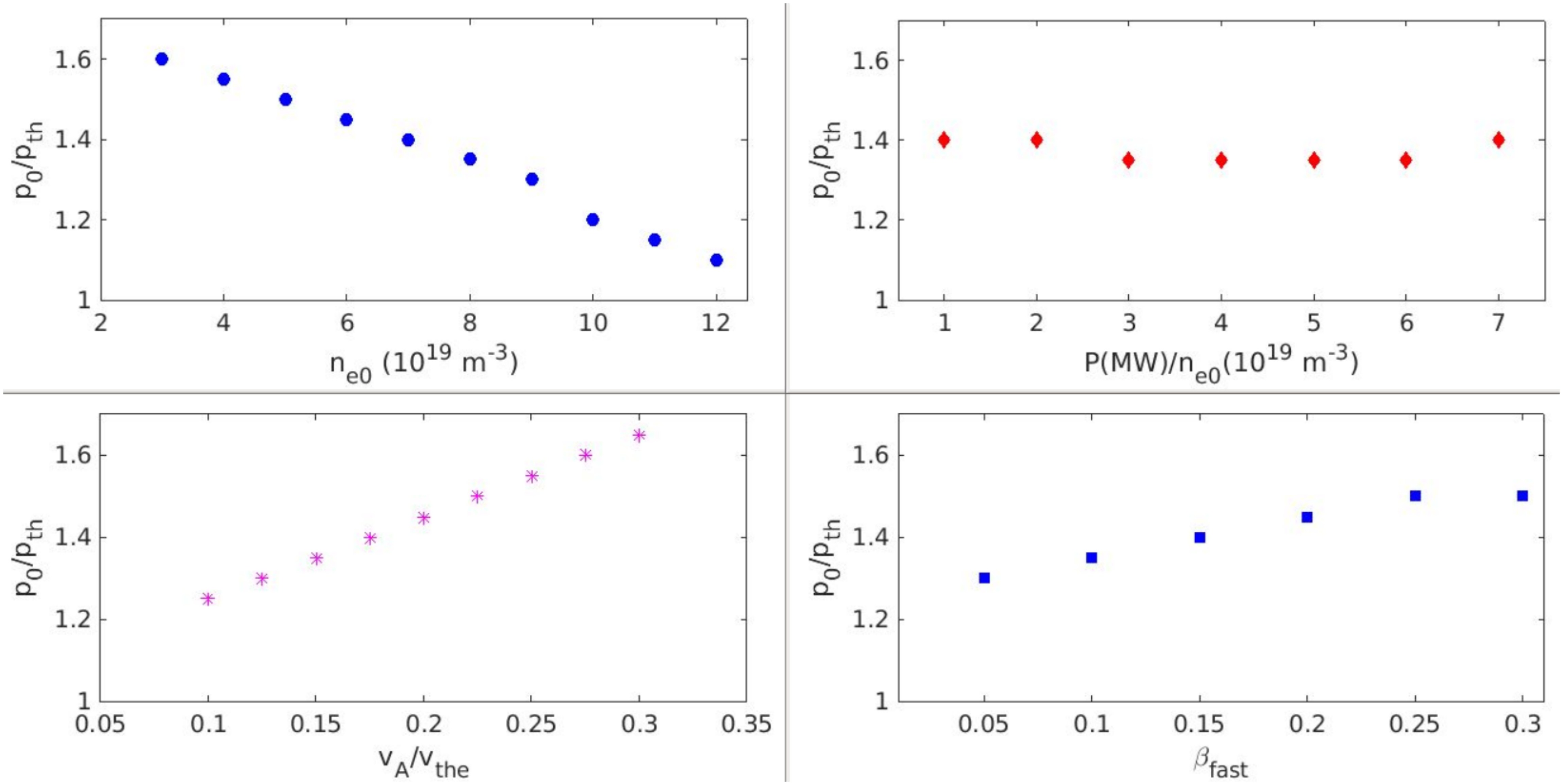

Landau damping of Kinetic Alfvén Waves in the Magnetosheath

- *S.A. Horvath et al., Phys. Plasmas **27**, 102901 (2020)*
- Gyrokinetic simulations of KAW absorption by the electrons in the Earth's magnetosheath
- **Bipolar signature** of Landau damping of KAW found in computations

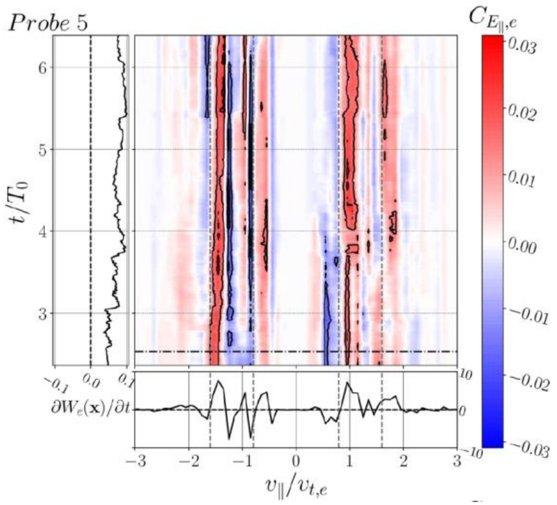

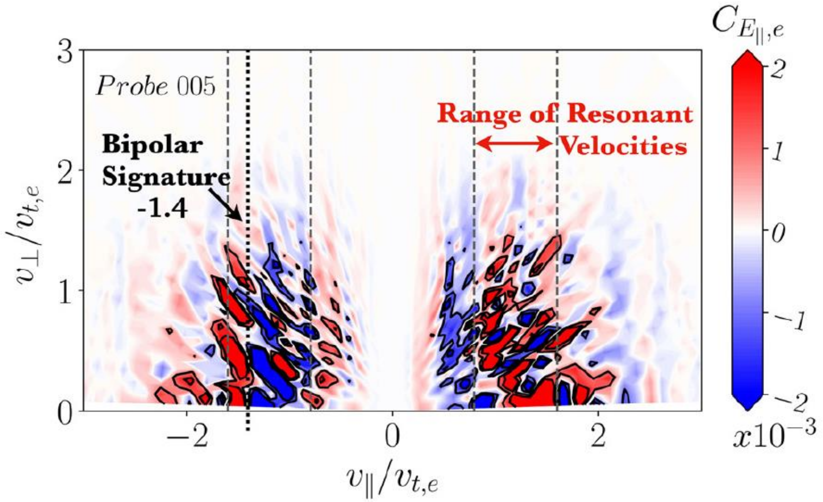

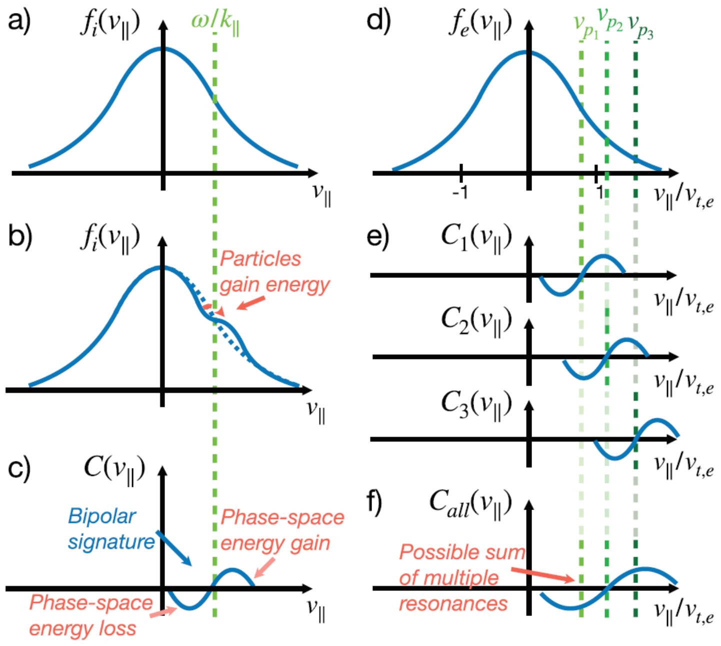

*C.H.K. Chen et al., Nat. Commun. **10**, 740 (2019)*

In-situ measurements of energy transfer from turbulence to electrons in the Earth's magnetosheath, from the Magnetospheric Multiscale (MMS) mission

Bipolar signature of Landau damping of KAW found in measurements